UNIVERSIDADE FEDERAL DO CEARÁ

CENTRO DE CIÊNCIAS

PROGRAMA DE PÓS-GRADUAÇÃO EM QUÍMICA

LLOYD RYAN VIANA KOTZEBUE

SPECTRAL AND THERMAL STUDIES ON THE SYNTHESIS AND OLIGOMERIZATION OF NOVEL CARDANOL-BASED BENZOXAZINES

FORTALEZA

2016

LLOYD RYAN VIANA KOTZEBUE

SPECTRAL AND THERMAL STUDIES ON THE SYNTHESIS AND OLIGOMERIZATION OF NOVEL CARDANOL-BASED BENZOXAZINES

Dissertação de mestrado apresentada ao Programa de Pós-graduação em Química, do Centro de Ciências da Universidade Federal do Ceará, como requisito parcial para obtenção do Título de Mestre em Química. Área de Concentração: Química Orgânica.

Orientador: Diego Lomonaco Vasconcelos de Oliveira

FORTALEZA

2016

Dados Internacionais de Catalogação na Publicação
Universidade Federal do Ceará
Biblioteca Universitária
Gerada automaticamente pelo módulo Catalog, mediante os dados fornecidos pelo(a) autor(a)

K1s Kotzebue, Lloyd Ryan Viana.
Spectral and thermal studies on the synthesis and oligomerization of novel cardanol-based benzoxazines / Lloyd Ryan Viana Kotzebue. – 2016.
76 f. : il. color.

Dissertação (mestrado) – Universidade Federal do Ceará, Centro de Ciências, Programa de Pós-Graduação em Química, Fortaleza, 2016.
Orientação: Prof. Dr. Diego Lomonaco Vasconcelos de Oliveira.

1. LCC. 2. cardanol. 3. polimerização térmica. 4. ROP. I. Título.

CDD 540

LLOYD RYAN VIANA KOTZEBUE

SPECTRAL AND THERMAL STUDIES ON THE SYNTHESIS AND OLIGOMERIZATION OF NOVEL CARDANOL-BASED BENZOXAZINES

Dissertação de mestrado apresentada ao Programa de Pós-graduação em Química, do Centro de Ciências da Universidade Federal do Ceará, como requisito parcial para obtenção do Título de Mestre em Química. Área de Concentração: Química Orgânica.

Aprovado em: 18/02/2016

BANCA EXAMINADORA

_____

Prof. Dr. Diego Lomonaco Vasconcelos de Oliveira (Orientador)

Universidade Federal do Ceará (UFC)

_____

Profa. Dra. Judith Pessoa de Andrade Feitosa

Universidade Federal do Ceará (UFC)

_____

Dra. Roselayne Ferro Furtado

Embrapa Agroindústria Tropical (EMBRAPA)

.

Dedicated to my sons, Christian and Adrian

Acknowledgements

To God for having guided me and given strength in my path as I needed. Thank you very much Lord.

To my wife Maruzia for her support and dedication that she gave and gives me every day. I love you.

To my parents for giving me love, support and for believing in me. I Love you.

To my sister who encouraged me and helped me in difficult times. Love you too.

To my advisor Prof. Diego Lomonaco for the great guidance he gave me along my Masters course. Thank you very much.

To Prof. Selma Elaine Mazzetto for the advice and support she gave me and for the opportunity to participate in the Laboratório de Produtos Tecnológicos e Processos (LPT).

To Prof. Judith for the good contributions in my research, as in my qualification as to allow to do the Gel Permeation Chromatography (GPC) analysis.

To my great friend Wanderson for the good working partnership, friendship and support.

To all the friends of LPT. You guys are amazing.

To Prof. Mele for the advises and for his big support with the mass spectrometry (MS) analysis.

To the funding agencies CNPq, CAPES and FUNCAP for financing my scholarship and research.

To Yara S. Oliveira, Prof. A. P. Ayala and the Laboratório de Caracterização e Crescimento de Cristais for the Differential Scanning Calorimetry (DSC) analyses.

To CENAUREMN (Centro Nordestino de Aplicação e Uso da Ressonância Magnética Nuclear) for the Nuclear Magnetic Ressonance (NMR) analyses.

“Knowing how to think empowers you far beyond those who know only what to think.”

Neil deGrasse Tyson

LIST OF FIGURES

LIST OF TABLES

RESUMO

Uma nova classe de polímeros que vem chamado atenção da indústria e da academia são as polibenzoxazinas, que podem ser obtidos após a polimerização térmica do seus monômeros, as benzoxazinas. Devido à grande versatilidade de síntese destes monômeros, que utiliza um composto fenólico e amina primária, possibilita-se o uso de fontes renováveis como o cardanol e a manipulação das propriedades do monômero e do polímero. Porém uma área pouco explorada é a compreensão da relação do tipo do material de partida utilizado com a síntese e polimerização das benzoxazinas. Desta forma, o objetivo deste estudo foi investigar como diferentes estruturas de aminas primárias influenciam na síntese e polimerização de novas benzoxazinas à base de cardanol. Os monômeros foram caracterizados e comparados utilizando RMN (^{1}H e ^{13}C), FT-IR, DSC e TGA. Demonstraram-se como aminas primárias influenciam na estabilidade do anel de oxazina, que se relaciona com a temperatura *onset* de polimerização (T_e). Benzoxazinas do tipo anilina proporcionam maior T_e do que as alifáticas. Sabendo que a alta T_e, cerca de 230 a 295 °C, poderia degradar a longa cadeia alquílica do cardanol, foram avaliados também a utilização de catalisadores, demonstrando o inócuo $MgCl_2$ ser um catalisador bastante promissor. A polimerização destes monômeros com $MgCl_2$ (1%) foi estudada utilizando FT-IR, DSC e GPC, mostrando que, de acordo com o comportamento de polimerização de cada benzoxazina, esta abordagem pode ser aplicada para uma melhor síntese de polibenzoxazinas à base de cardanol.

Palavras-chave: LCC. Cardanol. Polimerização térmica. ROP.

Abstract

A new class of polymers that is gaining attention of industry and academia are the polybenzoxazines, which can be obtained after the thermal polymerization of their monomers, benzoxazines. Due to the great versatility of the synthesis of these monomers, which uses a phenolic compound and primary amine, it is possible to use renewable sources such as cardanol and the manipulation of the monomer and polymer properties. However, an unexplored area is the understanding of the type of starting material used with the synthesis and polymerization of benzoxazines. Therefore, the aim of this study was to investigate how different primary amines structures influence on the synthesis and polymerization of novel cardanol-based benzoxazines. The monomers were characterized and compared using NMR (^{1}H and ^{13}C), FT-IR, DSC and TGA. It was demonstrated how primary amines influence on the stability of the oxazine ring, which relates to the onset polymerization temperature (T_e). Aniline-type benzoxazines provided higher T_e than aliphatic ones. Knowing that elevate T_e, around 230 to 295 ^{o}C, could degrade the long alkyl chain of cardanol, the use of catalysts was also evaluated, showing the innocuous $MgCl_2$ as very promising catalyst. The polymerization of these monomers with $MgCl_2$ (1%) were studied using FT-IR, DSC and GPC, showing that according to the polymerization behaviour of each benzoxazine, this approach can be applied successfully for a more effective synthesis of cardanol-based polybenzoxazines.

Keywords: CNSL. Cardanol. Thermal Polymerization. ROP.

LIST OF ABREVIATIONS AND SYMBOLS

CNSL Cashew Nut Shell Liquid

TGA Thermogravimetric Analysis

DSC Differential Scanning Calorimetry

FT-IR Fourier Transform Infrared Spectroscopy

ROP Ring Opening Polymerization

TLC Thin Layer Chromatography

$\mathbf{T_e}$ Onset Polymerization Temperature

$\mathbf{T_p}$ Peak Polymerization Temperature

$\Delta\mathbf{H_p}$ Enthalpy of Polymerization

$\bar{M}_n$ Number Average Molecular Weight

$\bar{M}_w$ Weight Average Molecular Weight

PDI Polydispersity Index

$\mathbf{x_n}$ Number Average Degree of Polymerization

$\mathbf{x_w}$ Weight Average Degree of Polymerization

SUMMARY

1. INTRODUCTION

1.1. Green Chemistry

Chemistry demonstrated to be very important for the development of the human civilization by satisfying their growing need of new sophisticated chemical products. From 1963 to 2013, the great development in medicine (pharmaceutical products) and in agriculture (crop protection products and fertilizers) made it possible to increase the world population from 3.2 to 7.2 billion people, combined with an increased life expectancy from 54 to 71 years (THE WORLD BANK, 2016)

On the other hand, Chemistry was also (or sometimes still is) seen by some of the society as the “science of toxic materials”, causing great damage on the human health and the environment. This is understandable due the fact that in the past, there wasn’t enough knowledge concerning the unfavourable consequences of chemicals. Nowadays, with the advancement of science in the last decades, there is a large collection of information of the malicious effects of a vast quantity of chemicals, which provides us to design a better process or product of our choice, minimizing as much as possible to harm the human health and environment.

Considering the environmental impacts and the finite resource of oil and petrochemical products, many efforts are being made to develop a more sustainable economy. Seeking this goal, Green Chemistry came as a new way of thinking for the development of chemical products and processes using its twelve principles (ANASTAS; WARNER, 1998), which are:

1. Waste prevention: waste must be prevented during the synthesis, leaving no residue to be cleaned or to be treated;
2. Designing safer products: designed product must be effective as possible for the desired function, possessing little or no toxicity;
3. Maximize energy efficiency: chemical reactions must be processed at room temperature and pressure when possible;
4. Less hazardous chemical syntheses: design syntheses were used reactants and generated products have low toxicity;
5. Use "green" solvents and auxiliaries: use more harmless auxiliary products possible when necessary. Use more environmentally friendly solvents possible;

6. Atom economy: synthesize that the final product has the maximum proportion of the starting reagents;
7. Use of catalysts: catalyst is required in small amounts for chemical reactions and they also avoid waste production;
8. Designing products to be degraded: the synthesized product should be degraded into harmless substances when discarded;
9. Analyse in real time to prevent pollution: monitor and control in real time to avoid all synthetic products;
10. Minimize the potential for accident: design a synthesis to prevent accidents;
11. Avoid chemical derivatives: avoid the most protective groups or other temporary modifiers, because they require additional steps which will generate more waste;
12. Use of renewable raw materials: using renewable materials instead of materials that are running out.

The use of renewable materials without hampering the food chain production is an ongoing concern around the globe. For this reason, agriculture residues are interesting feedstocks for the generation of "green" products that can possess similar or even better properties than its fossil origin. An already known renewable raw material which comply with these requirements is the Cashew Nut Shell Liquid (CNSL)

1.2. Cashew Nut Shell Liquid

Cashew nutshell liquid (CNSL) is the main by-product of the cashew nut (*Anacardium occidentale* L.) industries. Found in the honeycomb mesocarp of the cashew nutshell, this dark viscous liquid has a chemical composition of four phenolic compounds: anacardic acid, cardanol, cardol and 2-methylcardol (Figure 1). Due the rough thermal processes to obtain the cashew nut almond, the CNSL is now called as "technical CNSL", containing predominantly cardanol due the decarboxylation of anacardic acid (LOMONACO et al., 2012).

Figure 1 - Cashew nut shell liquid constituents

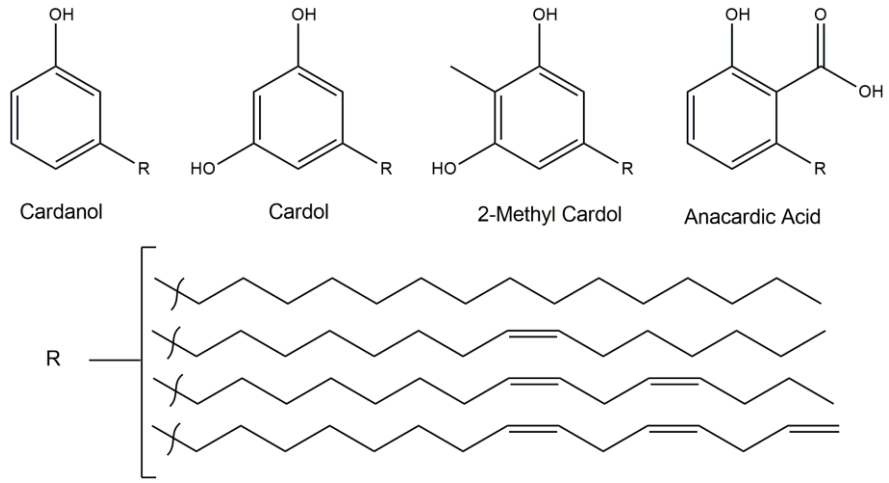

Source: The Author

Being aware that CNSL represent around 25% of weight of the nut, it was estimated that in 2013 (Graph 1) more than 1,000,000 tonnes of CNSL could be produced with the maximum total world production of 4,439,960 tonnes (FAO, 2015).

Graph 1 - World production of cashew nuts from 1993 to 2013

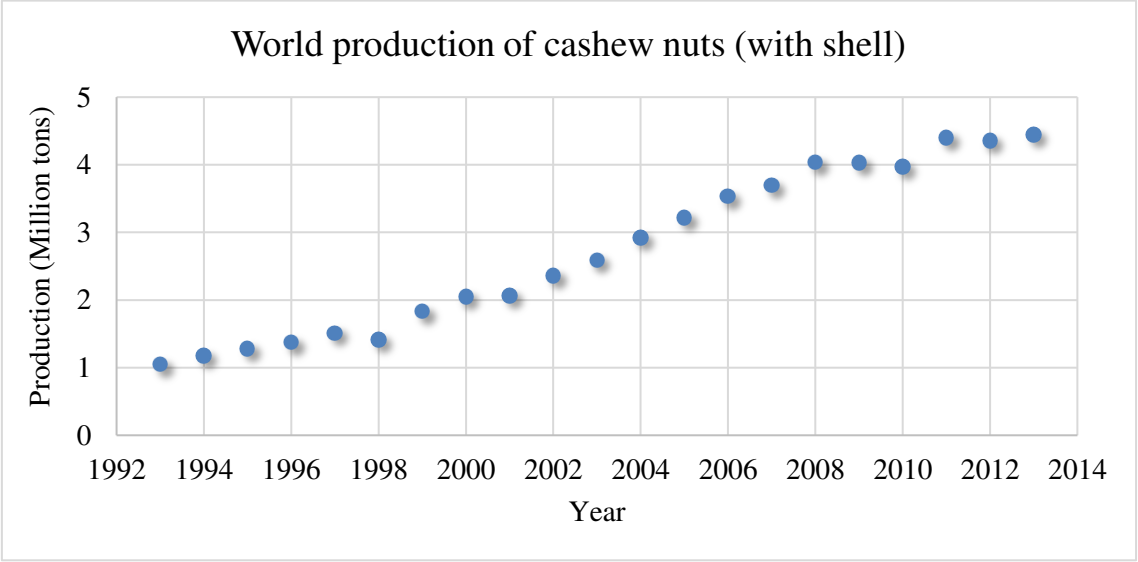

Source: FAO, 2015

Besides the biodegradability and its low cost, this enormous amount of natural phenolic compounds showed to be a very promising renewable feedstock for a variety of applications in the polymer industries where usually the fossil based phenols are used (MOHAPATRA; NANDO, 2014). Cardanol is already being used for the production of polyesters, polyurethanes (KATHALEWAR; SABNIS; D'MELO, 2014; TAWADE et al., 2014), phenolic resins, epoxy resins, polyols, (VOIRIN et al., 2014) and other bio-based polymers, like polybenzoxazines.

1.3. Benzoxazines

Benzoxazine is a benzene ring fused to an oxazine ring, a six-membered heterocycle constituted of one oxygen atom and one nitrogen atom. There are different kinds of isomeric benzoxazines which can vary on the oxidation of the oxazine ring and the positions of the heteroatoms. The 3,4-dihydro-*2H*-1,3-benzoxazine (Figure 2), which is commonly called among the academic and industrial communities as benzoxazine.

Figure 2 - Two types of benzoxazine molecules

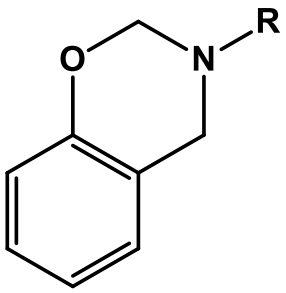

Benzoxazine
(3,4-dihydro-2*H*-1,3-benzoxazine)

Source: The Author

This type of molecule possesses a great molecular design flexibility which can be synthesized from a phenolic compound, a primary amine and two aldehydes (Figure 3a) (BARROSO et al., 2010), leading to a variety of benzoxazines as it can be observed on Figure 3b. For example, Li and co-workers synthesized a benzoxazine ferrocene group (1), giving this monomer electrochemical properties (LI et al., 2012).

Benzoxazines can be also synthesized with increased oxazine functionalities producing for example bis-benzoxazine (2 and 3) (LI et al., 2010) (SETHURAMAN; ALAGAR, 2015) or even multifunctional benzoxazine (4) (WANG et al., 2013b). Bio-based benzoxazines can also be generated from starting biochemicals, like Va-Bz (5), which was synthesized using as phenolic compound vanillin and as primary amine furfurylamine, derivate of furfural (SINI; BIJWE; VARMA, 2014). It is also possible to use different aldehydes for benzoxazine synthesis (6) (BARROSO et al., 2010), however, the use of formaldehyde has been reported more extensively (DENG et al., 2014a; DUMAS et al., 2013; LIU et al., 2011, 2015; LIU; ISHIDA, 2014; LOCHAB; VARMA; BIJWE, 2011; RUSSELL et al., 1998; SHARMA et al., 2014; WANG et al., 2014).

Figure 3 - Molecular design flexibility (a); and examples of some varieties of benzoxazines (b)

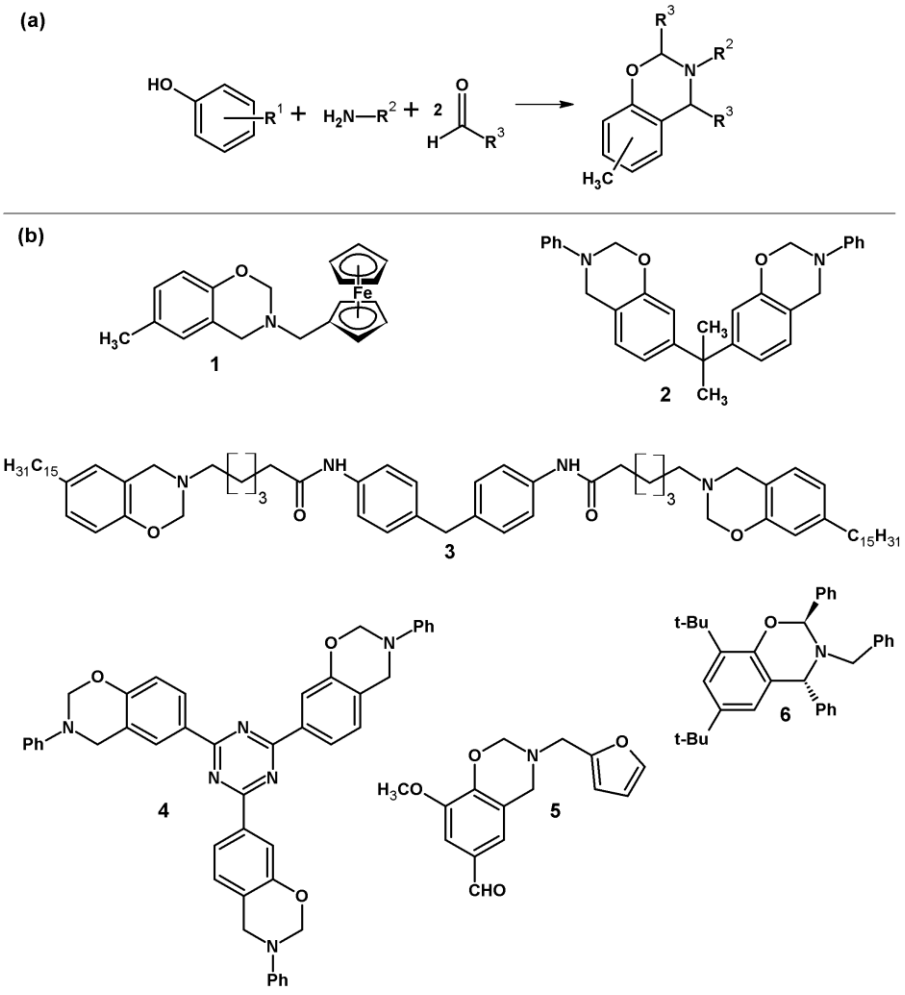

Source: The Author.

Mechanism of the benzoxazine synthesis is a Mannich-type reaction (Figure 4) that goes as follow. The primary amine reacts with the aldehyde to form a hemiaminal. Since the whole reaction is in equilibrium, the available protons from the reaction system is sufficient to catalyse the hemiaminal to form the imine. This imine will suffer an electrophilic aromatic substitution with the phenolic compound to form a Mannich bridge. The secondary amine group forms another imine, which is more electrophilic than the former, letting the hydroxyl group of the phenol be used as a nucleophile, generating the oxazine ring.

Figure 4 - Mechanism of the benzoxazine synthesis

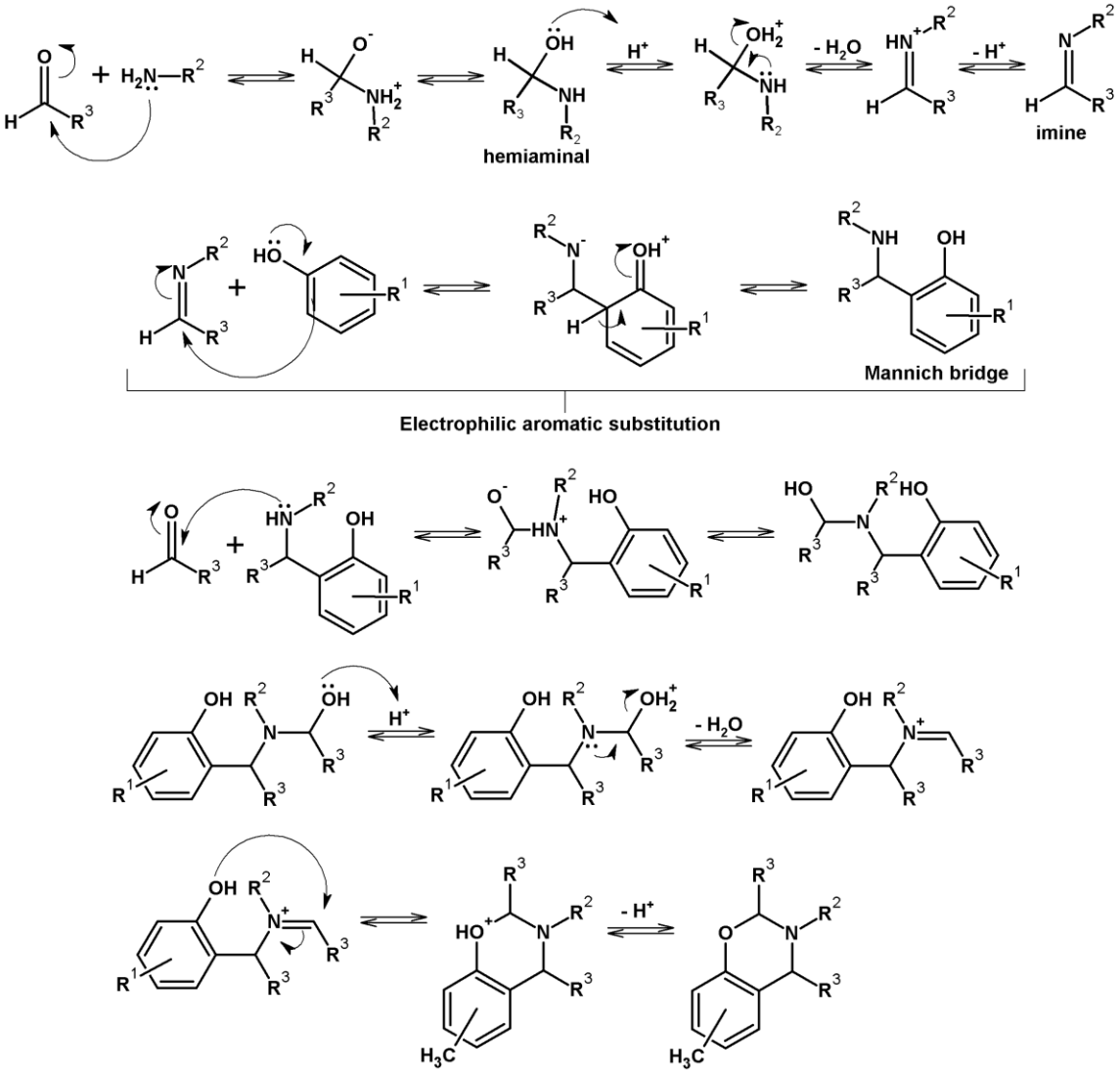

Source: The Author

Benzoxazines are receiving a lot of attention for biological systems because of the wide range of biological activities. Garg and co-workers synthesized benzoxazines derivatives as promising anticancer agents (GARG et al., 2013). Akhter and co-workers produced benzoxazines as anti-inflammatory and analgesic agents (AKHTER et al., 2011). Other biological activities of benzoxazines has also been reported to be used as fungicidal, antibacterial, antituberculosis, antihypertensive and many more (WANG et al., 2010). But in the last four decades, benzoxazines has attracted more attention as a promising resin precursor for the polymer industries.

1.4. Polybenzoxazines

The first reported syntheses of a benzoxazine monomer was in 1944 by Holly and Cope (HOLLY; COPE, 1944), not being studied as possible polymer precursor. Only in 1973, Schreiber noticed the formation of a hard and brittle material from benzoxazine, without studying the properties and the structure of the phenolic resin (ISHIDA; RODRIGUEZ, 1995). As the years pass by, more information was gathered of this new class of polymer, also known as polybenzoxazine.

Polybenzoxazines or benzoxazine resins have drawn a lot of attention due its unique advantages when compared with traditional phenolic resins, like: low dielectric constant; low water absorption; good thermal stability and chemical resistance; high mechanical properties; and no release of by-products during its thermal ring-opening polymerization (LOCHAB; VARMA; BIJWE, 2011; ZHANG et al., 2014).

The polymerization mechanism of benzoxazines is manly divided into two steps: the first is the opening of the oxazine ring after heat absorption; and second occurs the electrophilic substitution (Figure 5). The two main polymer structures are the phenoxy and phenolic types, being the latter thermodynamically more stable as demonstrated by Liu and co-workers (Liu et al., 2011). After polymerizing the benzoxazine at 200 °C for 2 hours, two polymeric structures can be obtained. After 4 hours of polymerization at the same temperature, only the phenolic structure was obtained.

Figure 5 - Basic polymerization mechanism of benzoxazines.

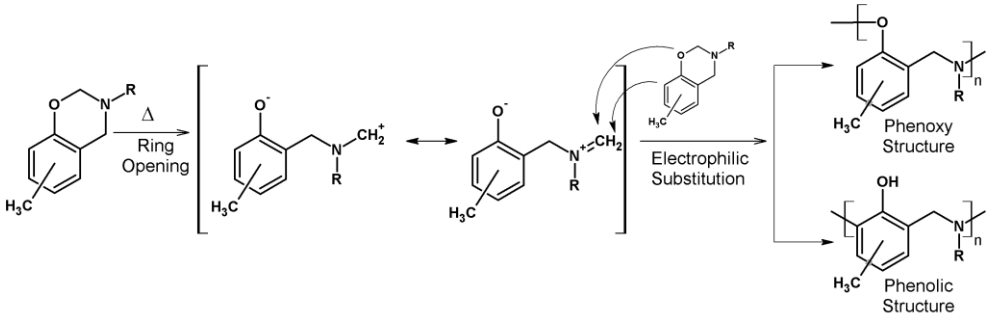

Source: The Author

1.4.1. Available benzoxazines for polymer and composite industries

Even though that many research already has been conducted in polybenzoxazines, they are still not easily available in the market. But some companies, like Huntsman, already provides a wide assortment of benzoxazines for a variety of applications in electronics, automotive, oil/gas and aerospace. Being one of the high performance components by the company, polybenzoxazines showed to be a very good alternative to the traditional epoxy, phenolic and bismaleimide (BMI) resins (Figure 6) (HUNTSMAN, 2016).

Figure 6 – Thermal performance/cost comparison of benzoxazine with traditional resins

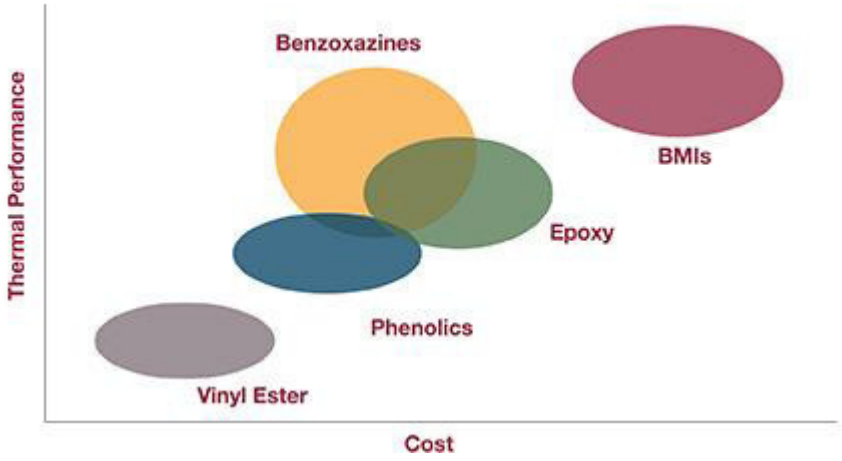

Source: (HUNTSMAN, 2016)

The polybenzoxazines are 50% stiffer than the epoxy resins, reaching flexural moduli in the range of 4,5 to 5,3 GPa. Using mainly bis-benzoxazines (Figure 7), there is no release of by-products during the curing process of the monomer, producing high quality laminates without voids. This makes the benzoxazine resins a better option than the phenolic resin, which are usually obtained by condensation reactions. Despite the fact that BMI resins possess the highest glass temperature (T_g), the use of autoclave with higher curing time make its producing cost much higher than that for polybenzoxazines (HUNTSMAN, 2016).

Figure 7 - Chemical structures of benzoxazine brands of Huntsman

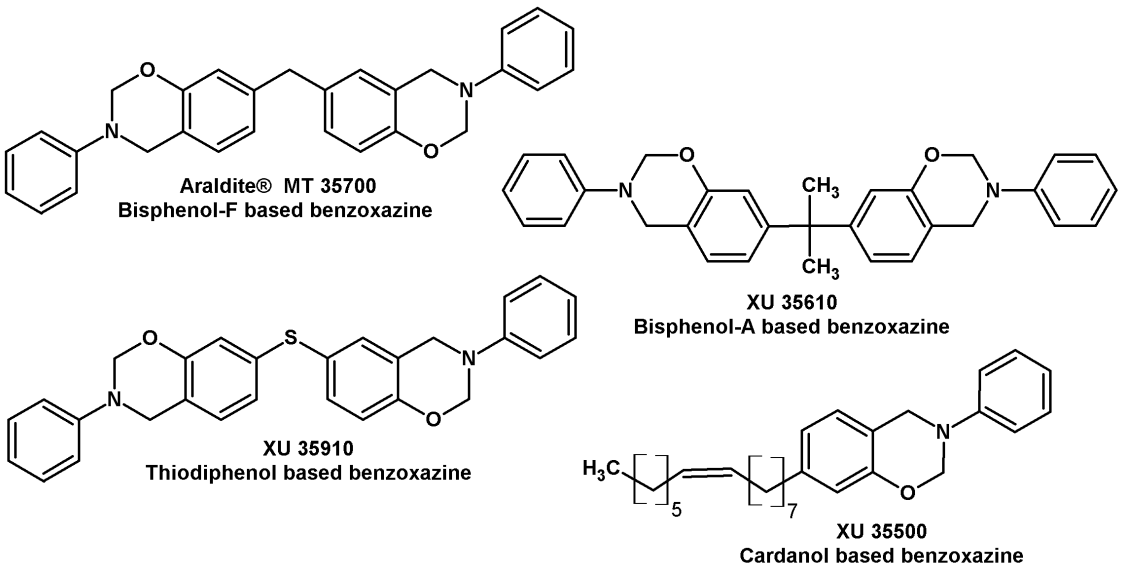

Source: The Author.

1.4.2. "Green" polybenzoxazines

Looking forward for the "green" benzoxazines production, the use of renewable phenolic compounds has been reported, such as urushiol, eugenol, guaiacol, vanillin and also cardanol, (CHIOU; ISHIDA, 2013; SINI; BIJWE; VARMA, 2014; THIRUKUMARAN; SHAKILA; MUTHUSAMY, 2014; WANG et al., 2012).

To our best knowledge, Rao and Pathak used cardanol to synthesize a phenylalkamine curing agent for the preparation of a copolymer network system with epoxide and a bis-benzoxazine (RAO; PATHAK, 2006). However, Caló and co-workers

developed the first cardanol-based benzoxazine and polybenzoxazine (CALÒ et al., 2007). Since then, cardanol was used as a fine bio-chemical for the synthesis of polybenzoxazines, proving that this phenolic compound is a very promising for this class of polymers (LI; LUO; GU, 2015; SETHURAMAN; ALAGAR, 2015; ZHANG et al., 2015).

In this work, it was studied the thermal and spectral behaviours of novel cardanol-based benzoxazines and its oligomers by varying the amine group. The thermal study was accomplished using differential scanning calorimetry (DSC) and thermogravimetry (TG). The spectral study was accomplished using nuclear magnetic resonance spectroscopy (NMR) and fourier transform infrared spectroscopy (FT-IR). The purpose of this study is to understand better the oligomerization behaviour of cardanol-based benzoxazines by modifying the amine group, for further applications of interest. Another interesting point discussed here is the utilization of catalysts to attenuate the ring-opening polymerization conditions, since polybenzoxazines are commonly produced under elevate temperatures, which may also cause partial degradation of the reagents. The molar weight distributions of these oligomers were also studied using gel permeation chromatography (GPC).

2. OBJECTIVES

2.1. General objective

Study the synthesis and the polymerization behaviour of bio-based benzoxazines by using cardanol as the main starting material, for a better design of cardanol-based benzoxazines for novel applications.

2.2. Specific objectives

- Synthesize five cardanol-based benzoxazines using the "solvent-free" method by using five different primary amines;
- Develop a purification method for cardanol-based benzoxazines by recrystallization using methanol as solvent;
- Characterize the benzoxazines by spectroscopic techniques like nuclear magnetic resonance (^{1}H NMR and ^{13}C NMR), by Fourier transformed infrared spectroscopy (FT-IR) and by mass spectrometry (MS);
- Analyse the thermal properties of the benzoxazines using differential scanning calorimetry (DSC) and thermogravimetric analysis (TGA);
- Study the thermal behaviour of the benzoxazines with different catalysts using differential scanning calorimetry (DSC);
- Study the polymerization process of each benzoxazines, containing the most ideal catalyst, through Fourier transformed infrared spectroscopy (FT-IR), differential scanning calorimetry (DSC) and gel permeation chromatography (GPC)

3. EXPERIMENTAL

3.1. Materials

The 3-*n*-pentadecylphenol (90-95%) was used as received from Acros Organics. Paraformaldehyde (95%), 4-chloroaniline (98%), tetrahydrofurfurylamine (97%), furfurylamine (> 99%), cyclohexylamine (99%) were used as received from Aldrich. Aniline (99%) and methanol (99,8%) were used from Vetec Química Fina.

3.2. General synthesis of benzoxazines

The method used for the cardanol-benzoxazine syntheses was an adapted method described by Attanasi and co-workers (ATTANASI et al., 2012).In a round bottom flask (125 mL) fitted with a condenser, 3-*n*-pentadecylphenol (2.96 mmol) and the primary amine (2.96 mmol) were heated under magnetic stirring at 70 °C. Paraformaldehyde (6.81 mmol) was added to this homogeneous molten mixture and then refluxed for three hours at 100 ºC. The progress of the reaction was followed by thin layer chromatography (TLC). After the completion of the reaction, the product was recrystallized using two different solvents. In the round bottom flask was added 20 mL of methanol and the mixture was stirred for 5 min. After stopping the magnetic stirrer, the supernatant was transferred to a 125 mL erlenmeyer. This procedure was repeated another four times. After collecting the supernatants, 1 mL of distilled water was added to this mixture and was put slowly to cool down till -4 °C for 90 minutes. After vacuum filtration, followed by washing with 5 mL of cold methanol, the obtained white product was placed inside the fumehood for 24 h for solvent evaporation.

3.3. Analytical methods

3.3.1. ^{13}C and ^{1}H Nuclear Magnetic Resonance Spectroscopy (^{1}H NMR and ^{13}C NMR)

The ^{1}H NMR and ^{13}C NMR spectra were recorded on BRUKER spectrometer, model Avance DPX, operating at frequencies for ^{1}H at 300 MHz and for ^{13}C at 75 MHz. Deuterated chloroform ($CDCl_3$) was used as solvent to solubilize the samples and tetramethylsilane (TMS) was used as an internal standard.

3.3.2. Fourier Transformed Infrared Spectroscopy (FT-IR)

The FT-IR spectra were obtained on a Perkin Elmer spectrometer, model FT-IR / NIR FRONTIER. Coaddition of four scans were recorded, using KBr windows with a resolution of 4 cm^{-1}, in the range of wavenumbers of 4000 to 400 cm^{-1}.

3.3.3. Mass Spectrometry Analysis

Mass spectrometry analysis were performed using an LC mass spectrometer Agilent 6540 Accurate-Mass Q-TOF equipped with an electrospray ionization interface working in positive ionization mode. The samples dissolved in a chloroform/acetonitrile solution were introduced in the mass spectrometer injected by an auto sampler using as eluent solution water (with added 0.1% HCOOH)/acetonitrile 10:90 (v/v) at a flow rate of 0.3 mL/min.

3.3.4. Differential Scanning Calorimetry Analysis (DSC)

The DSC thermograms were performed in a device of Mettler-Toledo, model DSC 823e, conducted under N_2 atmosphere (flow rate of 50 mL/min). For the characterization of monomers, the non-isothermal thermograms were obtained with a heating rate of 10° C/min, in a temperature range of 30 to 400° C, using approximately 5 mg of samples. All the analyses were performed using aluminium crucibles.

3.3.5 Thermogravimetry

TG thermograms were performed with a METTLER-TOLEDO equipment, model TGA/SDTA 851e, conducted under N_2 atmosphere (flow rate of 50 mL/min) with a heating rate of 10 °C/min in a temperature range of 30 to 800 °C. Alumina crucibles were used with approximately 5 mg of samples.

3.3.6 Polymerization of the benzoxazines

Approximately 50 mg of monomers were put in separate aluminium crucibles and then put simultaneously in an oven at 150 ºC under air for different polymerization times (1, 3, 5 and 7 h).

3.3.7 Gel Permeation Chromatography (GPC).

The molecular weight of the synthesized products was estimated by gel permeation chromatography using a Shimadzu LC-20AD chromatograph with refractive index detector RID-10A. The analyses were performed using Phenogel Linear column (7.8 × 300 mm), flow 1.0 mL / min, with toluene as the eluent, maintained in oven at 40 ° C. The injected sample volume was 20 µL. To construct the calibration curve, polystyrene Shodex SM-105 samples were used as standards.

3.3.8 Chromatographic Analysis

The thin layer chromatography (TLC) were carried out using silica gel plates supported on aluminium 60F254 manufactured by Merck, being revealed by exposure to ultraviolet (UV) irradiation at two wavelengths (254 and 365 nm) emitted by lamp model VL -4.LC of Vilber Lourmat. One benzoxazine was purified by column chromatography, using as stationary phase silica gel 60 (63 - 200 mm), manufactured by Vetec Química and as mobile phase eluent mixtures of hexane and ethyl acetate.

3-phenyl-7-pentadecyl-3,4-dihydro-2H-1,3-benzoxazine (CA-a)

^{1}H NMR (300 MHz, $CDCl_3$) δ 7.29 (dt, *J* =7.3Hz, *J* = 2.0 Hz, 2H), 7.15 (dd, *J* = 8.7 Hz, *J* = 1.1 Hz 2H), 6.96 (m, 1H), 6.94 (d, *J* = 7.9, 1H), 6.75 (dd, *J* = 7,7 Hz, *J* = 1.5 Hz, 1H), 6.67 (d, *J* = 1.4 Hz, 1H), *5*.36 (s, 2H), 4.63 (s, *2*H), 2.53 (t, *J* = 7.7 Hz, 2H), 1.59 (m, 2H), 1.28 (s,25H), 0.91 (t, *J* = 6.7 Hz, 3H). **^{13}C NMR** (75 MHz, $CDCl_3$) δ 154.24, 148.35, 143.33, 129.47, 126.64, 121.82, 121.41, 118.53, 117.98, 116.85, 79.65, 50.49, 35.85, 32.13, 31.50, 29.90, 29.87, 29.78, 29.70, 29.57, 29.52, 22.90, 14.32. **FT-IR** (cm^{-1}): 3029, 2956, 2917, 2849, 1622, 1602, 1576, 1499,1480, 1367, 1228, 1199, 1174, 1033, 942. **m.p.**: 64,6 – 66,3 ºC. ***m/z***: 422.3417 $(M + H)^+$

3-(4-chlorophenyl)-7-pentadecyl-3,4-dihydro-2H-1,3-benzoxazine (CA-ch)

^{1}H NMR (300 MHz, $CDCl_3$) δ 7.23 (d, *J* =9 Hz, 2H), 7.09 (d, *J* = 9 Hz, 2H), 6.93(d, *J* = 7.7, 1H), 6.76 (d, *J* = 7.7 Hz, *J* = 1.4 Hz, 1H), 6.67 (s, 1H), 5.30 (s, 2H), 4.60 (s, *2*H), 2.53 (t, *J* = 7.6 Hz, 2H), 1.58 (m, 2H), 1.27 (s,25H), 0.89 (t, *J* = 6.3 Hz, 3H). **^{13}C NMR**

(75 MHz, $CDCl_3$) δ 153.92, 147.01, 146.55, 143.74, 126.68, 121.83, 120.20, 117.28, 116.94, 79.73, 50.79, 35.88, 32.15, 31.49, 29.92, 29.90, 29.80, 29.72, 29.59, 29.54, 22.92, 14.34. **FT-IR** (cm^{-1}): 3033, 2955, 2918, 2850, 1622, 1597, 1579, 1497,1463, 1365, 1265, 1209, 1185, 1179, 1146, 1100, 1049, 1033, 942. **m.p.**: 72,2 - 73,2 ºC. ***m/z***: 456.3024 $(M + H)^+$

3-cyclohexyl-7-pentadecyl-3,4-dihydro-*2H*-1,3-benzoxazine (CA-cy)

^{1}H NMR (300 MHz, $CDCl_3$) δ 6.86 (d, *J* = 7.7, 1H), 6.69 (d, *J* = 7.7 Hz, 1H), 6.59 (s, 1H), 4.98 (s, 2H), 4.08 (s, *2*H), 2.72 (m, 1H), 2.52 (t, *J* = 7.5 Hz, 2H), 1.98 (m, 2H), 1.78 (m, 2H), 1.59 (m, 3H), 1.27 (s, 30H), 0.89 (t, *J* = 5.9 Hz, 3H). **^{13}C NMR** (75 MHz, $CDCl_3$) δ 154.93, 142.85, 126.90, 120.84, 118.68, 116.43, 80.23, 58.78, 47.44, 35.91, 32.12, 31.64, 31.54, 29.92, 29.90, 29.81, 29.74, 29.58, 26.07, 25.66, 22.91, 14.33. **FT-IR** (cm^{-1}): 3009, 2956, 2918, 2850, 1620, 1574, 1505, 1470, 1330, 1261, 1242, 1230, 1127, 1113, 1105, 940. **m.p.**: 45,0 – 46,2 ºC. ***m/z***: 428.3887 $(M + H)^+$

3-furfuryl-7-pentadecyl-3,4-dihydro-*2H*-1,3-benzoxazine (CA-fu)

^{1}H NMR (300 MHz, $CDCl_3$) δ 7.42 (d, *J* = 0.8 Hz, 1H), 6.87(d, *J* = 7.7, 1H), 6.73 (d, *J* = 7.6 Hz, 1H), 6.66 (s, 1H), 6.35 (dd, *J* = 2.6 Hz, *J* = 1,9 Hz, 1H), 6.28 (d, *J* = 2.9 Hz, 1H), 4.88 (s, 2H), 4.01 (s, *2*H), 3.95 (s, 2H), 2.54 (t, *J* = 7.6 Hz, 2H), 1.60 (m, 2H), 1.27 (s,25H), 0.89 (t, *J* = 6.0 Hz, 3H). **^{13}C NMR** (75 MHz, $CDCl_3$) δ 153.85, 151.70, 143.31, 142.84, 127.59, 121.38, 116.74, 116.44, 110.43, 109.31, 81.88, 49.63, 48.39, 35.93, 32.16, 31.57, 29.92, 29.89, 29.83, 29.76, 29.59, 29.58, 22.92, 14.34. **FT-IR** (cm^{-1}): 3024, 2957, 2917, 2849, 1621, 1578, 1506, 1471, 1445, 1247, 1170, 1143, 1128, 1113,1106, 944. **m.p.**: 78,2 – 81,6 ºC. *m/z*: 426.3368 $(M + H)^+$

3-tetrahydrofurfuryl-7-pentadecyl-3,4-dihydro-*2H*-1,3-benzoxazine (CA-thf)

^{1}H NMR (300 MHz, $CDCl_3$) δ 6.86 (d, *J* = 7.5, 1H), 6.69 (d, *J* = 7.5 Hz, 1H), 6.62 (s, 1H), 4.98 (s, 2H), 4.90 (m, 1H), 4.07 (s, *2*H), 3.90 (q, *J* = 7.0 Hz, 1H), 3.78 (q, *J* = 7.0 Hz, 1H), 2.91 (dd, *J* = 13.5 Hz, *J* = 3.4 Hz, 1H), 2.79 (dd, *J* = 13.5 Hz, *J* = 8.0 Hz, 1H), 2.52 (t, *J* = 7.5 Hz, 2H), 1.97 (m, 2H), 1.88 (m, 2H), 1.59 (m, 2H), 1.27 (s, 25H), 0.89 (t, *J* = 5.9 Hz, 3H). **^{13}C NMR** (75 MHz, $CDCl_3$) δ 154.151, 143.032, 127.496, 120.968, 117.395, 116.289, 83.345, 68.302, 56.167, 50.992, 35.883, 32.116, 31.527, 29.870, 29.847, 29.777, 29.711, 29.549, 29.524, 25.659, 22.877, 14.292. **FT-IR** (cm^{-1}): 2954,

2914, 2848, 1622, 1577, 1507, 1467, 1329, 1244, 1170, 1133, 1144, 1064, 1031, 940. **m.p.**: 37,5 – 38,8 ºC. ***m/z***: 430.3683 $(M + H)^+$

4. RESULTS AND DISCUSSION

4.1. Synthesis of cardanol-based benzoxazines

The monomers were obtained under solvent free conditions from saturated cardanol, paraformaldehyde and their respective primary amine as shown on Scheme 1. Due heat and using primary amine as base, the paraformaldehyde decomposes rapidly into formaldehyde. Once this carbonyl compound is available in the reaction media, the oxazine ring on the cardanol is formed through a Mannich-type reaction. For the best of our knowledge, among the synthesized benzoxazines, the ones derived from 4-chloroaniline (CA-ch), tetrahydrofurfurylamine (CA-thf), furfurylamine (CA-fu), and cyclohexylamine (CA-cy) are still unpublished compounds.

For purification of benzoxazines was designed, primarily, the use of column chromatography techniques. 1.53 g of the crude CA-a was purified by gravitational column chromatography using 1.4 L of total solvent mixture in different ratios (hexane / ethyl acetate) to give 0.963 g of CA-a (69%). Looking forward to reduce the use of large amounts of solvents to purify benzoxazines, an eco-friendlier purification method was sought. The recrystallization of benzoxazines proved to be a very effective method (BARROSO et al., 2010; SINI; BIJWE; VARMA, 2014; WANG et al., 2013b). However, as far as we know, it has not been reported recrystallization of cardanol-based benzoxazines. In this work, recrystallizations of these benzoxazines were performed using methanol as solvent.

The purification of the CA-a by recrystallization gave a yield of 61% which is slight lower than that obtained of column chromatography, but, the purity of the recrystallized monomer was higher than the other. This recrystallization showed to be a very efficient way to purify the monomer, since the amount of solvent used was greatly reduced from 1.4 L to approximately 100 mL.

After using the same purification method for the other benzoxazines, it is important to point out that the aliphatic benzoxazines, CA-cy and CA-thf, gave low yields of 41 and 43%. However, other benzoxazines containing aromatic amines, CA-ch and CA-fu, were better recrystallized giving yields of 72 and 74 %, respectively. This higher yield may be due the *pi*-stacking of the aromatic groups, which leads to better purifications of these monomers.

Scheme 1 - Reaction of cardanol-based benzoxazines

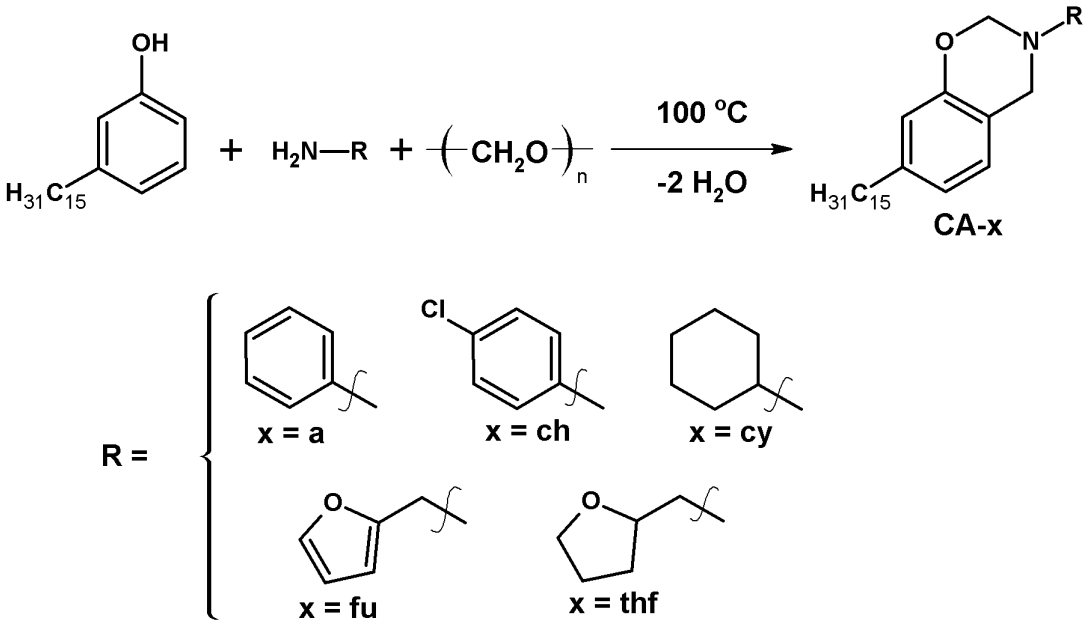

Source: The Author

4.2. Structure characterization of cardanol-based benzoxazines

4.2.1. ^{1}H and ^{13}C Nuclear Magnetic Resonance

Before comparing the ^{1}H and ^{13}C NMR spectra of the five cardanol-based benzoxazines between them, it is necessary to identify first the peaks that are common with each other (Figure 8).

Figure 8 - Main structure of saturated cardanol-based benzoxazine

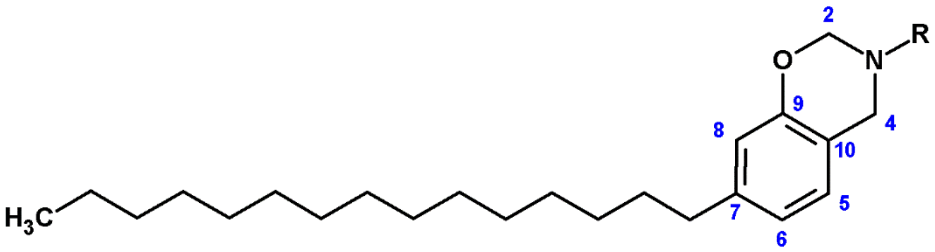

Source: The Author.

In the ^{1}H NMR spectra of the benzoxazines, three aromatic protons are quite similar or the same which are protons 8, 6 and 5. Proton 8 appears as a singlet at 6.62 ppm; proton 6 appears as a doublet at 6.69 ppm; and proton 5 appears also as a doublet at 6.86 ppm. The following peaks are attributed to the long alkyl chain of cardanol. The triplet at 2.53 ppm and the multiplet at 1.60 ppm refer to the methylene group attached to the phenolic ring and to the next methylene group, respectively. The terminal methyl group is represented as a triplet at 0.91 ppm and the long singlet at 1.28 ppm is attributed for the other methylene groups of the alkyl chain (LOMONACO et al., 2009). After identifying their similar peaks, two peaks are of most interest when it concerns to characterization of benzoxazines, which represents the two methylene groups of the oxazine ring.

In the ^{13}C NMR spectra of the benzoxazines, there were found similar peaks between them referring to the carbons of the phenolic ring of the monomers. The oxygenated aromatic carbon 9 was found at 154.13 ppm and the C_{15}-alkyl substituted aromatic carbon 7 was attributed at 143.01 ppm. The peaks at 127.47, 120.95, 117.37 and 116.27 ppm are related to carbon 5, 6, 10 and 8. The signals regarding the alkyl chain are found between 36.00 and 13.00 ppm (LOMONACO et al., 2009).

The chemical shifts of the oxazinic methylenes, O-**CH_2**-N and Ar-**CH_2**-C, are found in the ^{1}H NMR in the region of 5.5 to 3.8 ppm and in the ^{13}C NMR in the region of 85 to 49 ppm (ISHIDA; AGAG, 2011).

After understanding the main signals of the ^{1}H NMR and ^{13}C NMR spectra of the cardanol-based benzoxazine, the following interpretation of spectra will be simplified.

3-phenyl-7-pentadecyl-3,4-dihydro-*2H*-1,3-benzoxazine (CA-a)

In the ^{1}H NMR spectrum (Figure 9) of the CA-a , it was observed the aromatic hydrogen absorption by the following chemical shifts: the doublet of triplet at 7.29 ppm (J = 7.3 Hz, J = 2.0 Hz) is assigned to the hydrogen 13; a doublet of doublet at 7.15 ppm (J = 8.7 Hz, J = 1.1 Hz) represents hydrogen12; the multiplet at 6.96 ppm refers to hydrogen 14; the doublet at 6.94 ppm (J = 7.9 Hz) refers to hydrogen 5; a doublet of doublet at 6.75 ppm (J = 7.7 Hz, J = 1.5 Hz) attributed to hydrogen is 6; the doublet at 6.67 ppm (J = 1.4 Hz) refers to the proton 8. Two singlets were observed at 5.36 ppm

and 4.63 ppm, which are related to the oxazinic methylenes, O-**H**$_2$-N and Ar- **H**$_2$-C, respectively.

Figure 9 - ^{1}H NMR spectrum of CA-a

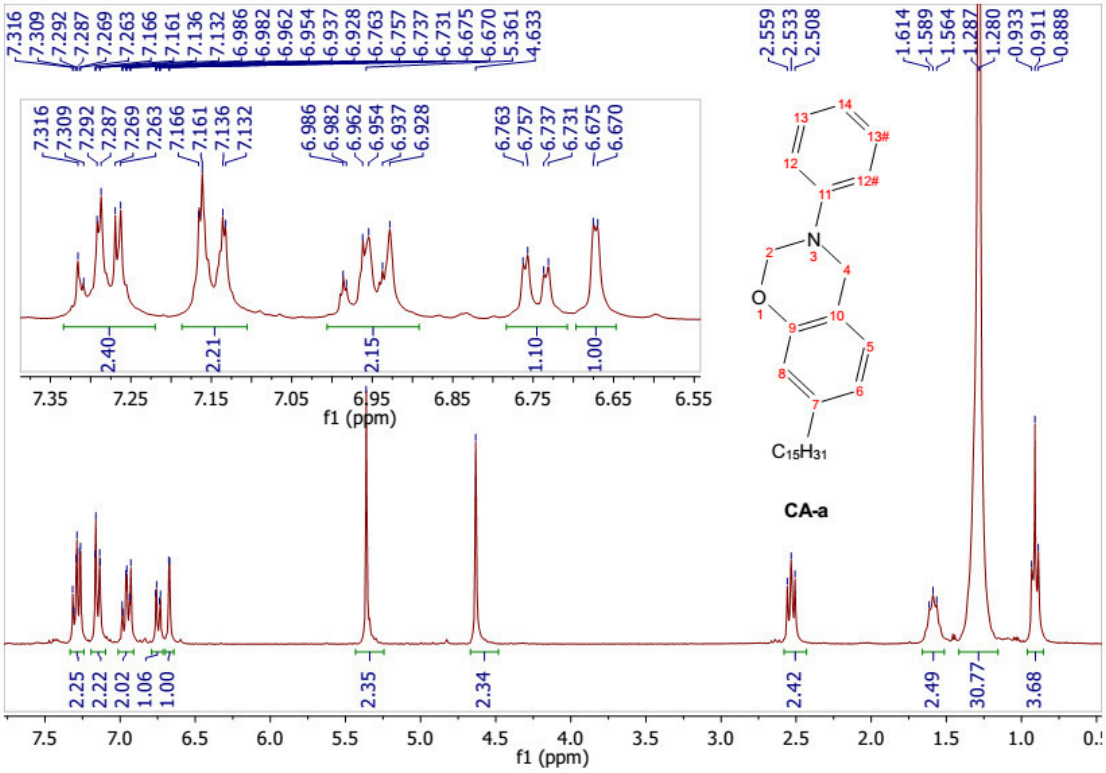

Source: The Author

In the ^{13}C-NMR spectrum (Figure 10) of CA-a, the absorptions of aromatic carbons could be observed by the following chemical shifts: the peak at 154.24 ppm was assigned to the oxygenated carbon 9; the substituted carbon 11 containing the amino group was found in 148.35 ppm; it was observed a peak at 143.33 ppm which was attributed to the alkyl substituted carbon 7; the peaks of carbons 13, 12, 14 were observed at 129.47, 118.53 and 117.98 ppm, respectively; the peak at 116.85 ppm was assigned to the carbon 8; the peaks at 126.64, 121.82 and 121.41 ppm are related to carbons 5, 10 and 6, respectively. It was also observed the absorptions of the oxazinic carbons, O-**CH**$_2$-N and Ar-**CH**$_2$-N with the peaks in 79.65 and 50.49 ppm, respectively.

Figure 10 - ^{13}C NMR spectrum of CA-a

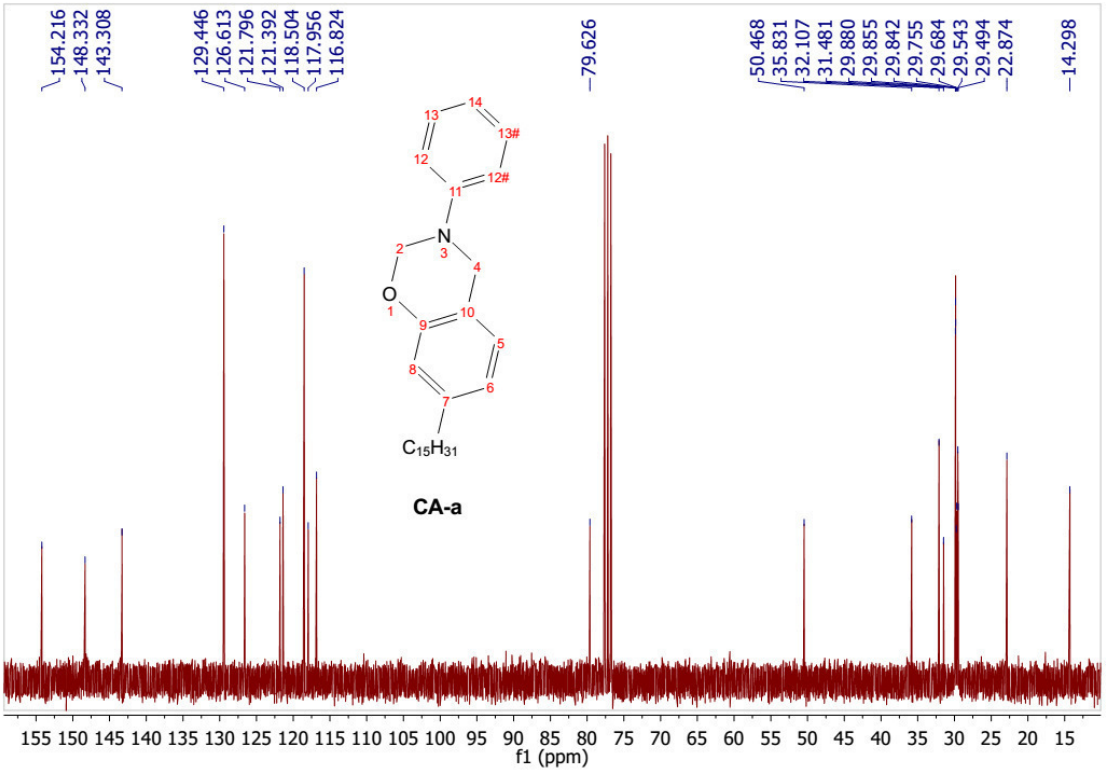

Source: The Author

3-(4-chlorophenyl)-7-pentadecyl-3,4-dihydro-*2H*-1,3-benzoxazine (CA-ch)

In the ^{1}H NMR spectrum (Figure 11) of CA-ch, it was observed the aromatic hydrogen absorption by the following chemical shifts: the doublet at 7.23 ppm (J = 9 Hz) refers to hydrogen 13; the doublet at 7.09 ppm (J = 9 Hz) attributed to hydrogen is 12; the absorption of hydrogen 5 was found as a doublet at 6.93 ppm (J = 7.7 Hz); a doublet of doublet at 6.76 ppm (J = 7.7 Hz, J = 1.4 Hz) is attributed to hydrogen 6; a singlet at 6.67 ppm is assigned to hydrogen 8. Also, two singlets were observed at 5.30 ppm and 4.60 ppm which are related to methylenes O-**H**$_2$-N e Ar-**H**$_2$-N, respectively.

Figure 11 - ^{1}H NMR spectrum of CA-ch

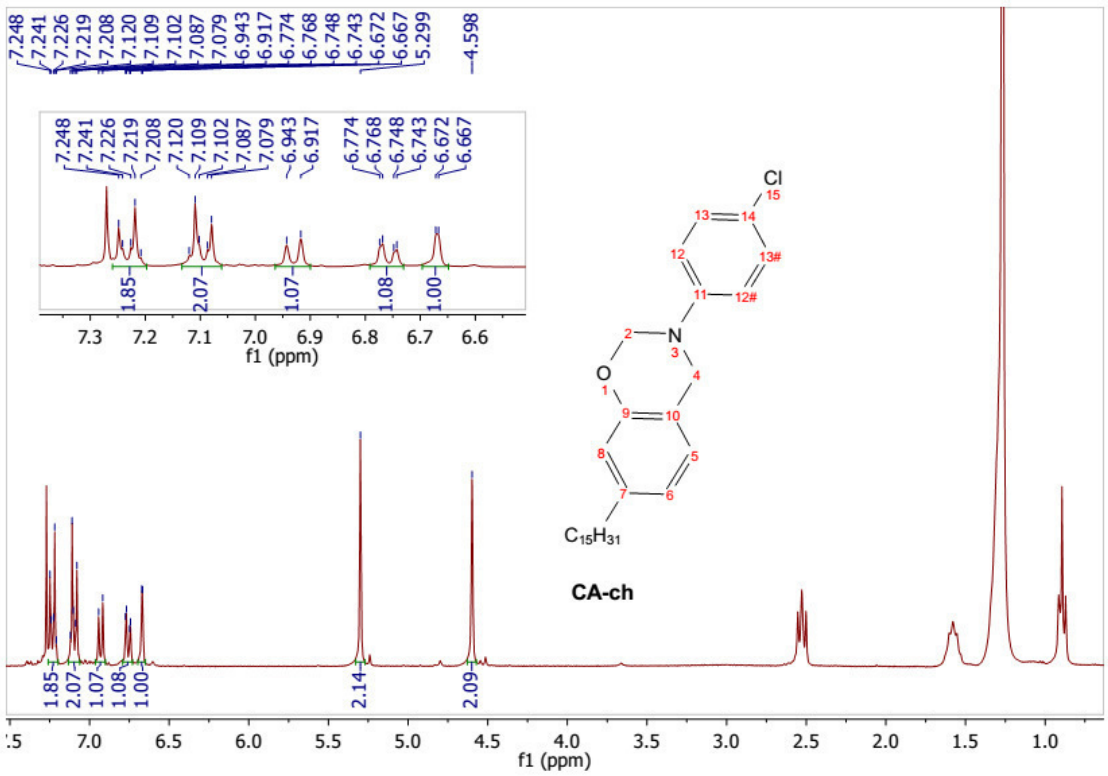

Source: The Author

In ^{13}C NMR spectrum (Figure 12) CA-ch, it was observed the absorption of aromatic carbons by the following chemical shifts: the peak at 153.92 ppm was assigned to the oxygenated carbon 9; the amino substituted carbon 11 was found 147.01 ppm; the carbon substituted with the chlorine atom 14 was found in 146.55 ppm; it was observed a peak at 143.33 ppm which referred to the alkyl substituted carbon 7; the peaks of the carbon 13 and 12 were observed at 129.51 and 120.20 ppm, respectively; The peak at 116.94 ppm was assigned to the carbon 8; The peaks at 126.68, 121.82 and 117.28 ppm are related to carbons 5, 10 and 6, respectively. It was also observed absorptions of the carbons of methylenes groups O-**CH$_2$**-N e Ar-**CH$_2$**-N peaks in the 79.73 and 50.79 ppm, respectively.

Figure 12 - ^{13}C NMR spectrum of CA-ch

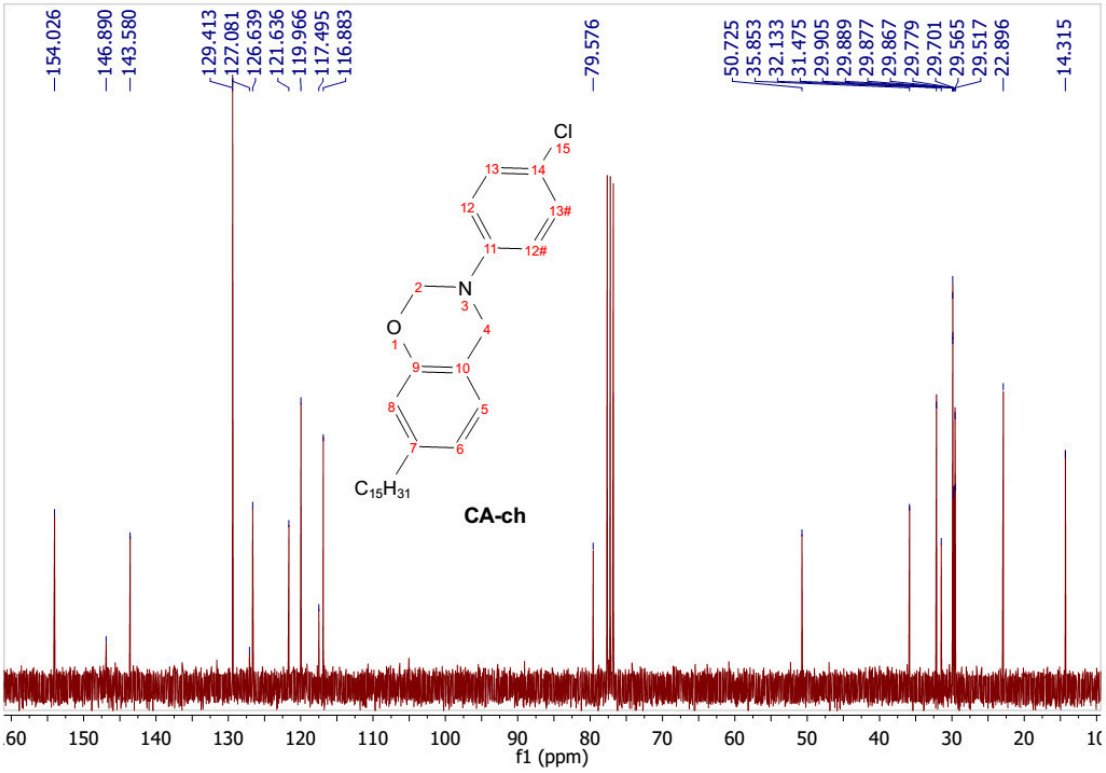

Source: The Author

3-cyclohexyl-7-pentadecyl-3,4-dihydro-*2H*-1,3-benzoxazine (CA-cy)

In the ^{1}H NMR spectrum (Figure 13) of CA-cy, it was observed the aromatic hydrogen absorption by the following chemical shifts: the doublet at 6.86 ppm (J = 7.7 Hz) refers to hydrogen 5; the doublet at 6.69 ppm (J = 7.7 Hz) refers to hydrogen 6; singlet at 6.59 ppm. refers to hydrogen 8. Also, two singlets were observed at 4.98 ppm and 04.08 ppm which are related to the methylenes O-**CH**$_2$-N e Ar-**CH**$_2$-N, respectively. The remaining peaks are attributed to the alkyl groups of the amine group and of the phenolic group.

Figure 13 - ^{1}H NMR spectrum CA-cy

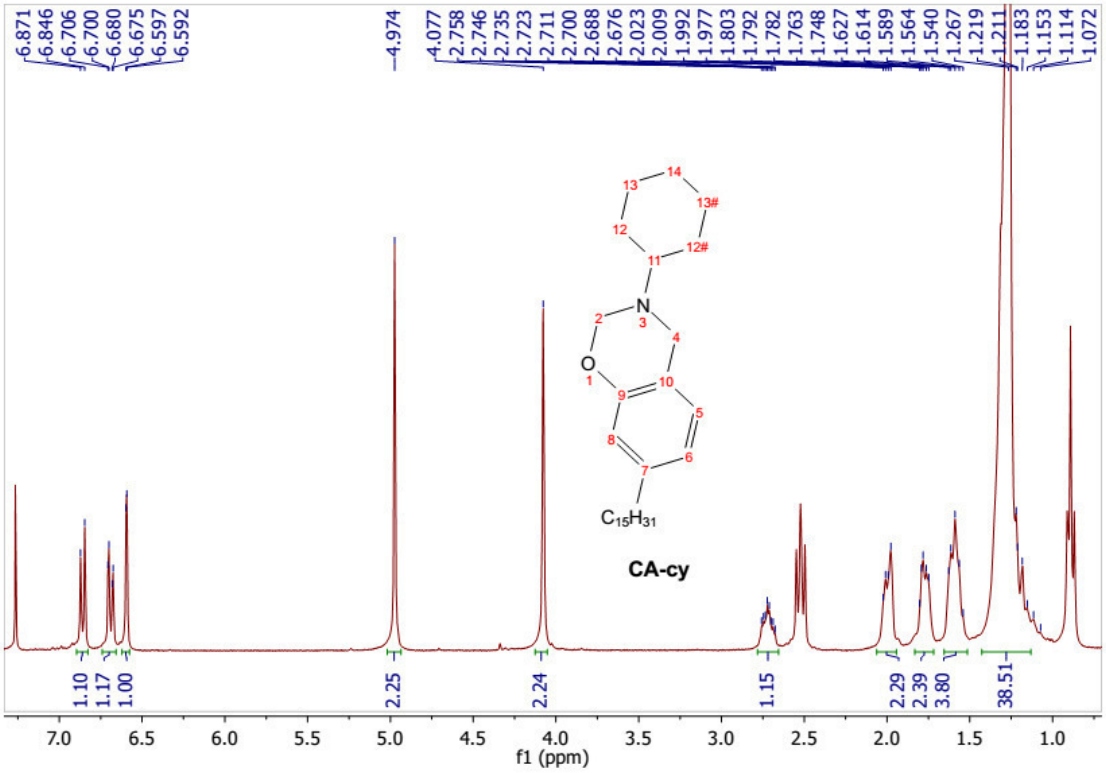

Source: The Author

In ^{13}C NMR spectrum (Figure 14) of CA-cy, it was observed the absorption of the aromatic carbons by the following chemical shifts: the peak at 153.93 ppm was assigned to the oxygenated carbon 9; a peak at 142.85 ppm was observed which was assigned to alkyl substituted carbon 7; the peak at 116.43 ppm was assigned to the carbon 8; the peaks at 126.90, 120.82 and 118.68 ppm are related to carbons 5, 10 and 6, respectively. It was also observed absorptions of the carbons of methylenes groups, O-**CH$_2$**-N e Ar-**CH$_2$**-N, on the peaks in 80.23 and 47.44 ppm, respectively. Signals between 48-14 ppm refer to the carbons of the cyclic group of primary amine and alkyl chain.

Figure 14 - ^{13}C NMR spectrum of CA-cy

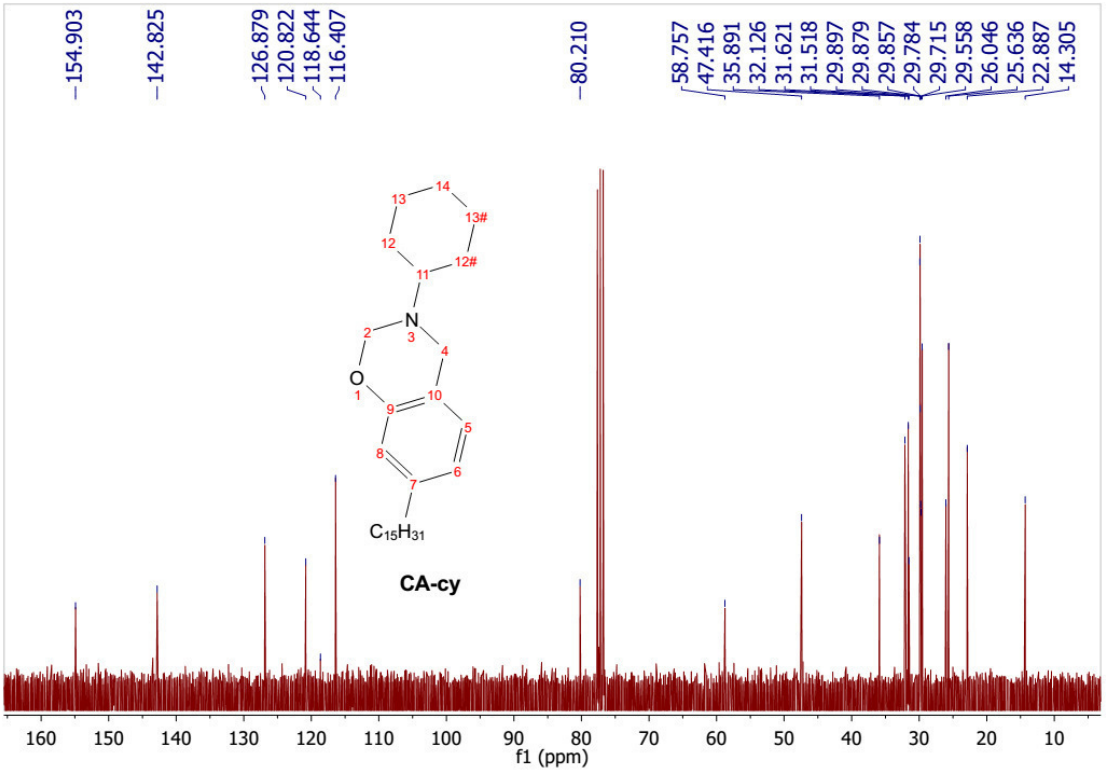

Source: The Author

3-furfuryl-7-pentadecyl-3,4-dihydro-*2H*-1,3-benzoxazine (CA-fu)

In the ^{1}H NMR spectrum (Figure 15) of CA-fu, it was observed the aromatic hydrogen absorption by the following chemical shifts: the doublet at 7:42 ppm (J = 0.8 Hz) refers to protons 12; the doublet at 6.87 ppm (J = 7.7 Hz) refers to proton 5; the doublet at 6.73 ppm (J = 7.6 Hz) refers to the proton 6; the singlet at 6.66 ppm refers to the proton 8; the doublet of doublet at 6:35 ppm (J = 2.6 Hz, J = 1.9 Hz) is attributed to the hydrogen 13 and the doublet at 6.28 ppm (J = 2.9 Hz) refers to hydrogen 14. It was also observed two singlets at 4.88 ppm and 4.01 ppm which are related to methylenes O-**H**$_2$-N e Ar-**H**$_2$-N, respectively. The methylene amino group has been found as a singlet at 3.95 ppm.

Figure 15 - ^{1}H NMR spectrum CA-fu

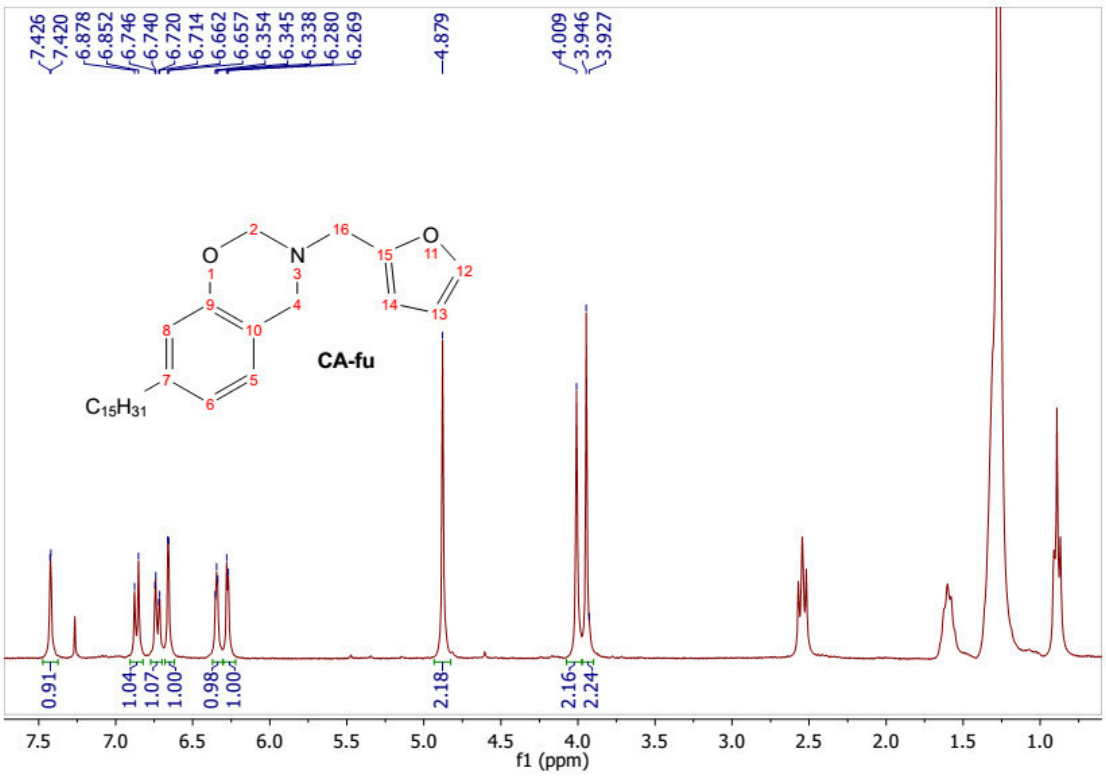

Source: The Author

In the ^{13}C NMR spectrum (Figure 16) CA-fu, it was observed the absorption of aromatic carbons by the following chemical shifts: the peak at 153.85 ppm was assigned to the oxygenated carbon 9 and the peak at 151.70 ppm was assigned to oxygenated carbon 15; the oxygenated carbon 12 was assigned to the peak at 143.31 ppm; a peak was observed at 142.84 ppm which referred to the alkyl substituted carbon 7; The peak at 116.44 ppm was assigned to the carbon 8; the peaks at 127.59, 121.38 and 116.74 ppm were related to carbon atoms 5, 10 and 6, respectively. The peaks at 110.43 and 109.31 ppm are assigned to the carbons 13 and 14. It was also observed the absorptions of the carbons of methylenes groups O-**CH$_2$**-N e Ar-**CH$_2$**-N at 81.88 and 49.63 ppm, respectively. The methylene of the amino group has been found by the peak at 48.39 ppm

Figure 16 - ^{13}C NMR spectrum of CA-fu

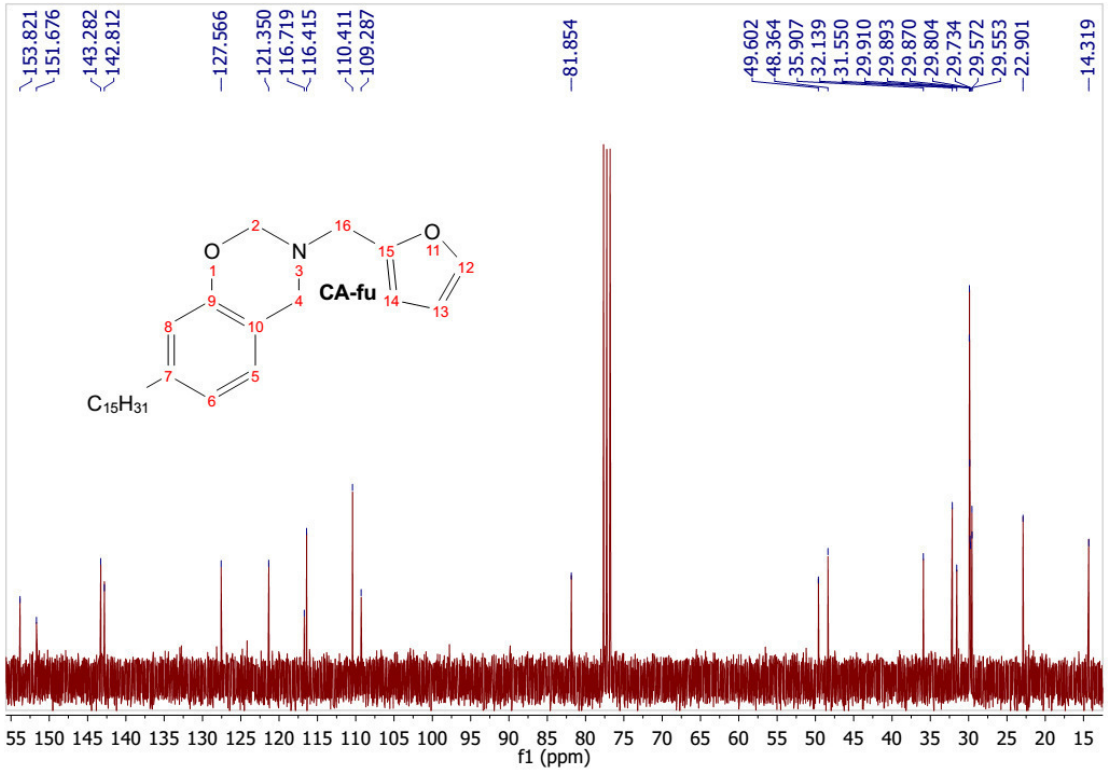

Source: The Author

3-tetrahydrofurfuryl-7-pentadecyl-3,4-dihydro-*2H*-1,3-benzoxazine (CA-thf)

In the ^{1}H NMR spectrum (Figure 17) CA-thf, it was possible to observe the aromatic hydrogen absorptions by the following chemical shifts: the doublet at 6.86 ppm (J = 7.5 Hz) refers to the proton 5; the doublet at 6.69 ppm (J = 7.5 Hz) refers to the proton 6; the singlet at 6.62 ppm refers to proton 8. Also, two singlets were observed at 4.98 ppm and 4.07 ppm which are related to methylenes O-**H$_2$**-N e Ar-**H$_2$**-N, respectively. The signs for the tetrahydrofurfuryl group were assigned the following chemical shifts: the singlet at 4.90 ppm was assigned to the hydrogen of the stereogenic carbon; quartets at 3.90 and 3.78 ppm were attributed to methylene hydrogens 12; the two doublets of doublets at 2.91 and 2.79 ppm represent methylene linked with tetrahydrofuran. The two multiplets at 1.97 and 1.88 ppm represents the hydrogens 13 and 14.

Figure 17 - ^{1}H NMR spectrum CA-thf

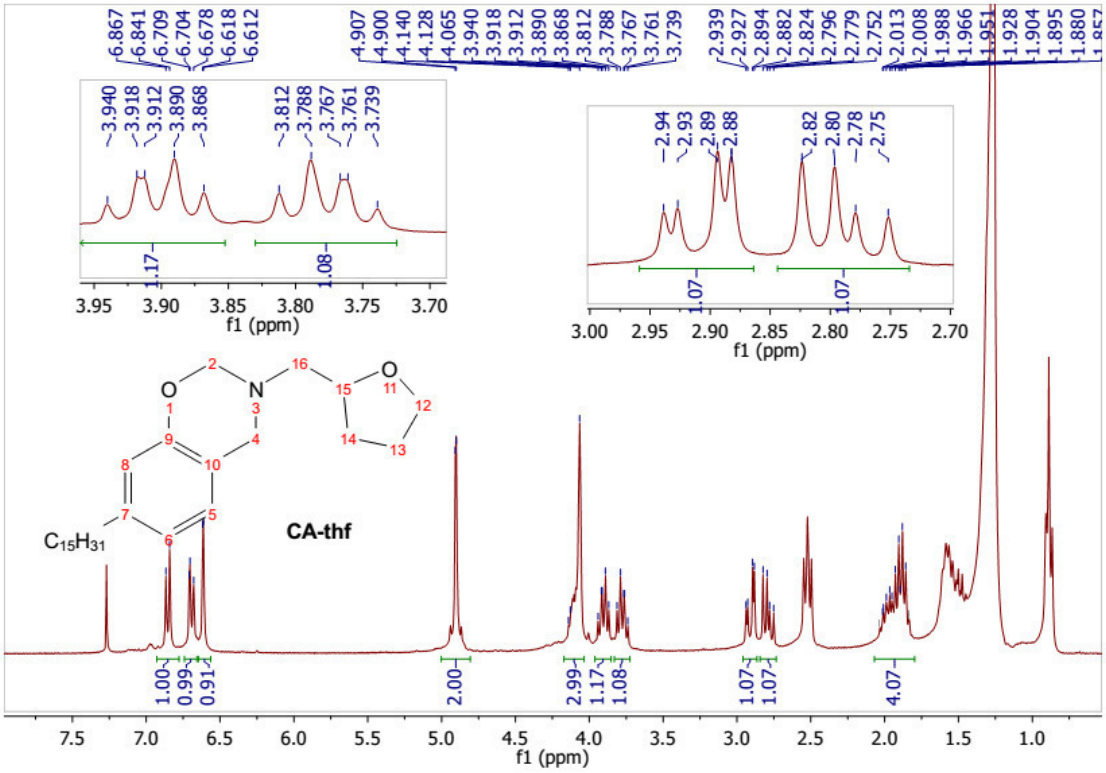

Source: The Author

In the ^{13}C NMR spectrum (Figure 18) of CA-thf, it was observed the absorptions of aromatic carbons by the following chemical shifts: the peak at 154.15 ppm was assigned to the oxygenated carbon 9; it was observed a peak at 143.03 ppm which referred to alkyl substituted carbon 7; the peak at 116.29 ppm was assigned to the carbon 8; the peaks at 127.50, 120.97 and 117.40 ppm are related to carbons 5, 10 and 6, respectively. It was also observed absorptions of the carbons of the methylenes groups O-**CH$_2$**-N e Ar-**CH$_2$**-N by the peaks at 83.35 and 56.17 ppm, respectively. The absorptions of the two oxygenated carbons of the tetrahydrofuran group 15 and 12 were observed at 68.30 and 56.17 ppm, respectively.

Figure 18 - ^{13}C NMR spectrum of CA-thf

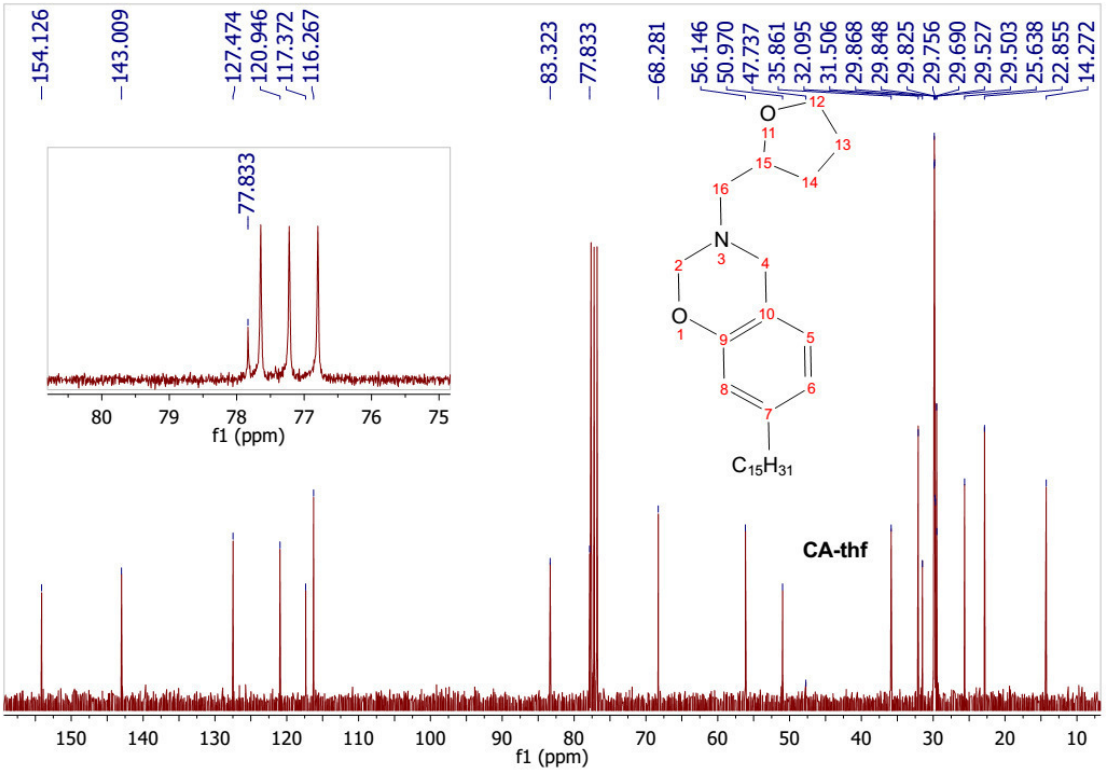

Source: The Author

The oxazinic methylene groups, O-**CH₂**-N and the Ar-**CH₂**-N, of the cardanol-based benzoxazines were found at around 5,40 to 4,80 **(a)** and 4,65 to 3,99 ppm **(b)**, respectively (Figure 19). The reason why the oxazinic methylene hydrogens of aniline-derivates benzoxazines are less shielded than the others is due the electron withdrawing resonance effect of the nitrogen atom with the benzene ring. In the resonance structures of these aniline-derivative benzoxazines, the nitrogen atom possesses a positive partial charge, reducing the electron density on the oxazinic hydrogens.

Figure 19 - ^{1}H NMR spectra of the cardanol-based benzoxazines

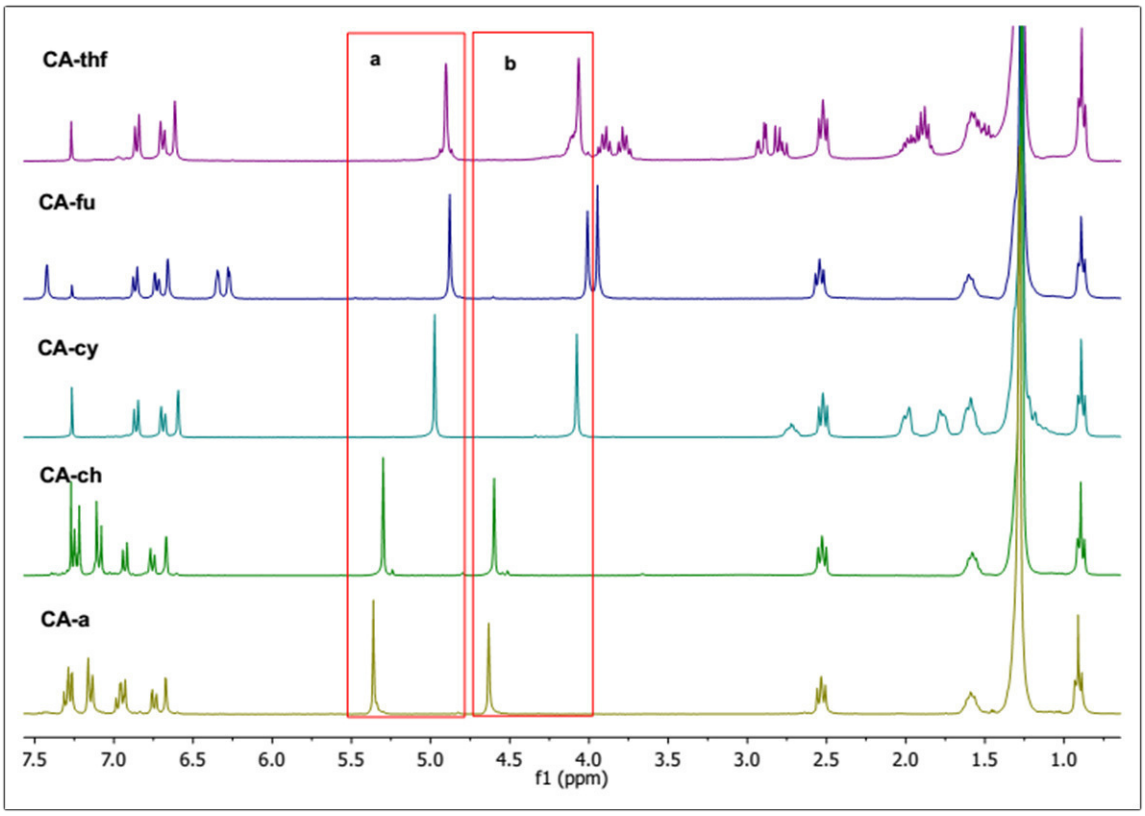

Source: The Author

Comparing the chemical shifts of the ^{1}H and ^{13}C NMR spectra of the oxazinic methylene groups of the presented compounds, it was observed that the protons O-**CH$_2$**-N and Ar-**CH$_2$**-N of the benzoxazines containing primary amines derived from aniline (CA-a and the CA-ch) were less protected than the others in the ^{1}H NMR spectra. This observation is the opposite in the ^{13}C NMR spectra (Figure 20), where the oxazinic methylene carbons of CA-a and the CA-ch are more shielded than the others.

Figure 20 - ^{13}C NMR spectrum of the cardanol-based benzoxazines

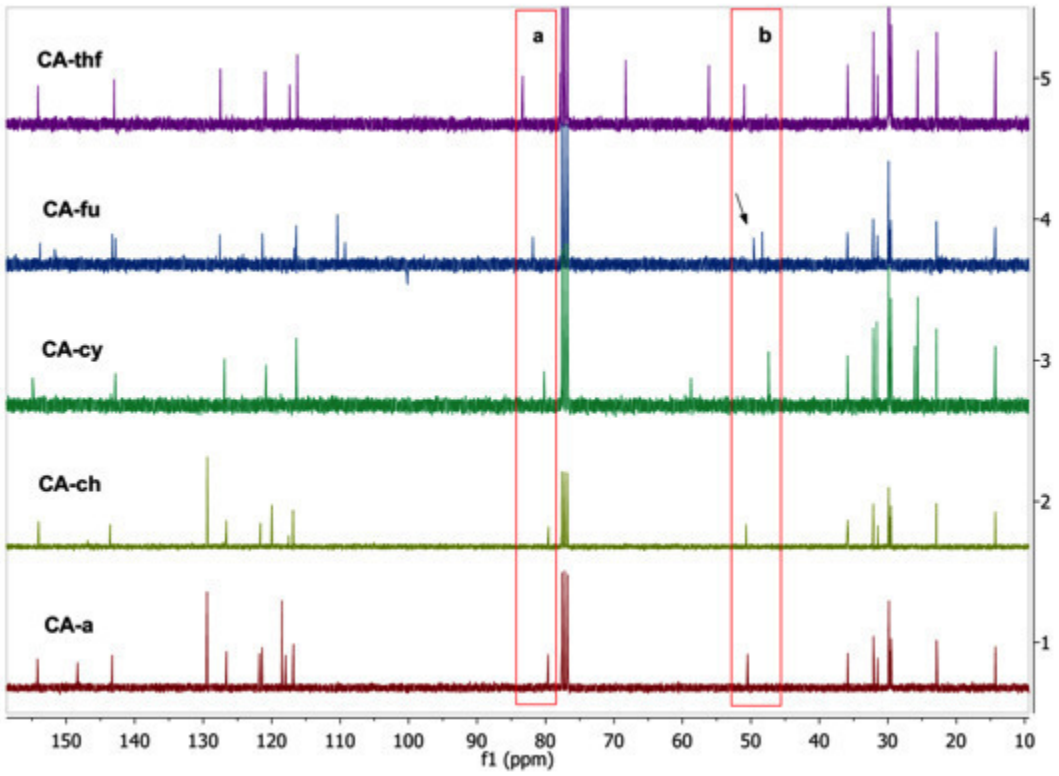

Source: The Author

4.2.2. Fourier transform infrared spectroscopy (FT-IR)

Another widely used spectral characterization method to study benzoxazines is Fourier transform infrared spectroscopy (FT-IR), being more specific in the fingerprint region. This range is usually of most interest, especially when analysing the polymerization behaviour of the monomers.

By comparing the FT-IR spectra of the five cardanol-based benzoxazines (Figure 21 and Table 1), some similarities and differences were found between them. The bands at around 1620 and 1576 cm^{-1} indicated the C=C stretching of the benzene ring and the absorption band at 1600 cm^{-1} assigned to the C=C stretching of aniline-derivatives (CA-a and CA-ch). The characteristic mode of the C=C stretching of tri-substituted benzene ring was around 1498 cm^{-1} to benzoxazines containing aniline derivatives (CA-a and CA-ch) and 1506 cm^{-1} for the remaining benzoxazines (CA-cy CA-fu and CA-thf). The asymmetrical and symmetrical stretching =C-O-C occurred in bands between 1227-1262 cm^{-1} and 1020-1048 cm^{-1}, respectively. The band absorption

relative to the aryl C-Cl bond of CA-ch occurred in 1049 cm^{-1} (BARANEK et al., 2012; DUNKERS; ISHIDA, 1995; LIU; ISHIDA, 2014; WANG et al., 2014).

Figure 21 - FT-IR spectra of the cardanol-based benzoxazines in fingerprint region.

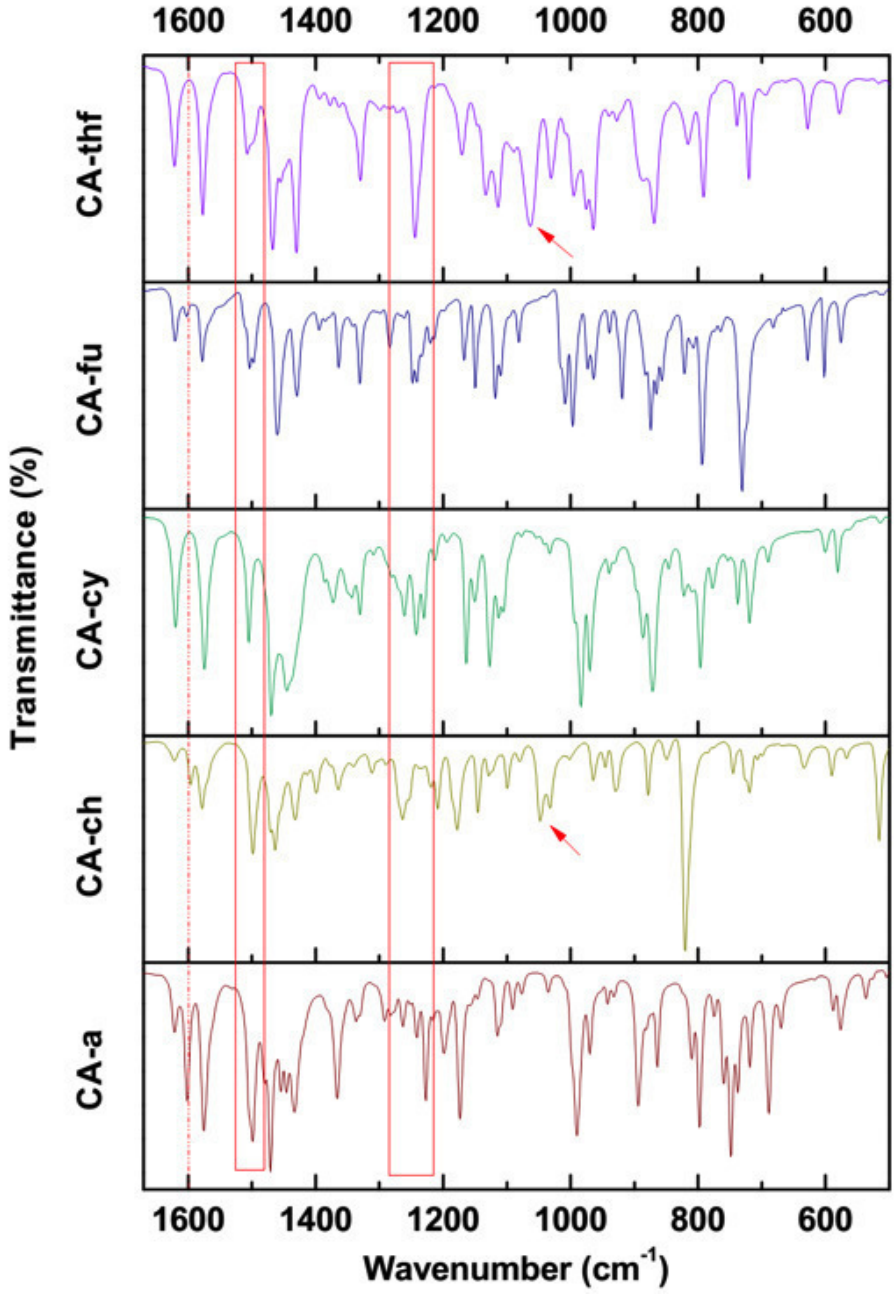

Source: The Author

Table 1 - Summary of the IR vibration modes of the cardanol-based benzoxazines.

CA-a		CA-ch		CA-cy		CA-fu		CA-thf		Vibrational mode
cm^{-1}	Int.	cm^{-1}	Int.	cm^{-1}	Int.	cm^{-1}	Int.	cm^{-1}	Int.	
1622	m	1622	w	1620	m	1621	m	1622	m	C=C stretching of benzene ring
1602	m	1597	m							C=C stretching of aniline-derivatives
1576	m	1579	m	1574	m	1578	m	1577	s	C=C stretching of benzene ring
1499	s	1498	s	1505	m	1506	m	1507	m	C=C stretching of tri-substituted aromatic ring
1228	m	1262	s	1242	m	1247	m	1245	s	=C-O-C asymmetric stretching
		1049	s							C-Cl stretching
								1063	s	C-O-C asymmetric stretching

Source: The Author

4.2.3. Mass Spectrometry Analysis

The experimental conditions used to perform the analyses by mass spectrometry (see analytical methods) were chosen to optimize the soft ionization by H^+ of the benzoxazines being these compounds quite unstable under hard ionization conditions. The molecular ion peaks both calculated and found for the cardanol based benzoxazines, reported in Table 2, are in agreement with the proposed structure completing the spectroscopic characterization of the monomeric benzoxazine derivatives.

Table 2 - Exact Mass expected and found for of the cardanol-based benzoxazines.

Benzoxazine	Molecular Formula	$[M+H]^+$ Expected (amu)	$[M+H]^+$ Found (amu)
CA-a	$C_{29}H_{43}NO$	422.3417	422.3417
CA-ch	$C_{29}H_{42}ClNO$	456.3028	456.3024
CA-cy	$C_{29}H_{49}NO$	428.3887	428.3887
CA-fu	$C_{28}H_{43}NO_2$	426.3367	426.3368
CA-thf	$C_{28}H_{47}NO_2$	430.3685	430.3683

Source: The Author

4.3. Thermal characterizations of the cardanol-based benzoxazines

4.3.1. Differential Scanning Calorimetry (DSC)

The polymerization behaviour of the monomers was analysed by performing non-isothermal differential scanning calorimetry (DSC) (Figure 22) and their data were summarized on Table 3.

Figure 22 - Non-isothermal DSC curves of the cardanol-based benzoxazines.

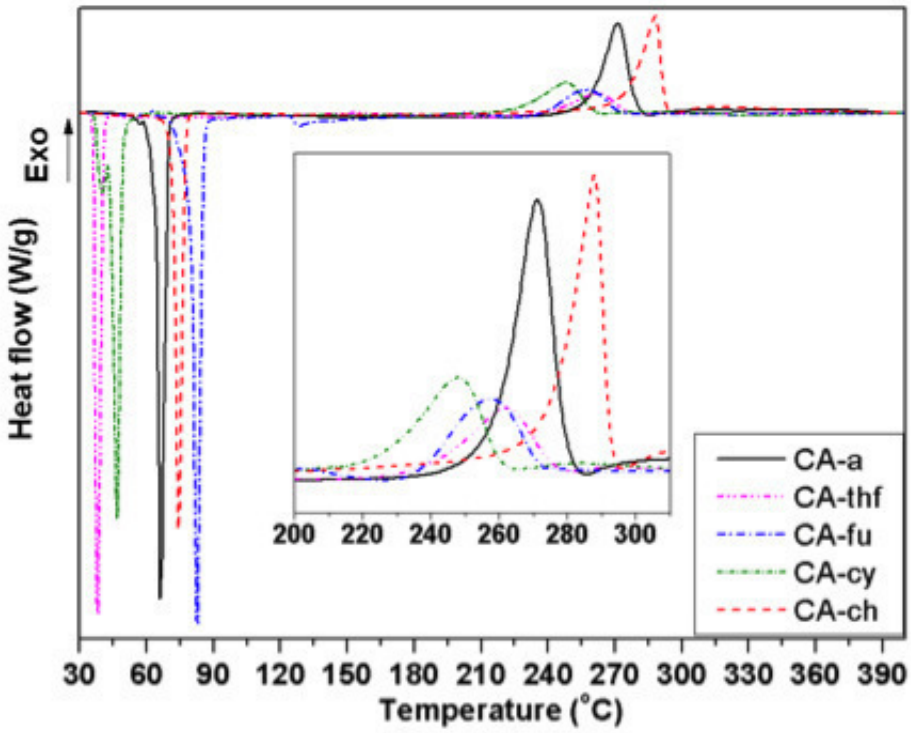

Source: The Author

Table 3 - Values obtained from the non-isothermal DSC thermograms of the benzoxazines**.**

Monomer	T_m (°C)	T_e (°C)	T_p (°C)	ΔH (Jg^{-1})
CA-a	66.2	260.6	271.6	-90.9
CA-ch	74.9	269.4	282.3	-90.3
CA-cy	49.0	233.7	250.3	-46.2
CA-fu	83.2	236.1	259.3	-40.1
CA-thf	40.5	241.3	259.6	-38.9

Source: The Author

The melting points (T_m) presented by the endothermic events of the benzoxazines containing aromatic amine groups were higher than those containing aliphatic amine groups. This observation is due to the *pi-pi* interactions of aromatic groups (e.g., parallel stacking off-centre interactions end-to-face) (MARTINEZ; IVERSON, 2012), which are stronger intermolecular forces than London forces.

The exothermic events indicate the temperature range at which the ring-opening polymerization occurs after the cleavage of the C-O bond of the oxazine ring. According to Deng and co-workers, the opening of the oxazine ring at higher temperatures indicates a greater stability of the ring, due to increased strength of C-O bond (DENG et al., 2014a). On the other hand, the stability of the oxazine ring is also dependent on the influence of the anomeric effect, which is related to the basicity of the amine group (Figure 23). The constructive interaction of nitrogen non-bonding orbital in parallel with the antibonding orbital of low energy C-O σ*, makes the C-O bond longer and weaker. When this bond is cleaved by heat absorption, the formed carbocation of the zwitterionic intermediate is stabilized by the sharing of the non-bonding electron pair of the nitrogen atom (LIU et al., 2015; RUSSELL et al., 1998). This explains why the CA-a, possesses a higher onset polymerization temperature than CA-cy, CA-fu and CA-thf. If the non-bonding electron pair of nitrogen is in resonance with the benzene ring, less stable will be the carbocation, strengthening the C-O bond. This same principle also explains why the onset polymerization temperature of CA-ch is about 10 °C higher than CA-a. The presence of chlorine in *para* position to the aniline

of CA-ch, performs an electron withdrawing effect on the nitrogen atom, stabilizing even more the oxazine ring than of the CA-a.

Figure 23 - The anomeric effect on 1,3-oxazine ring

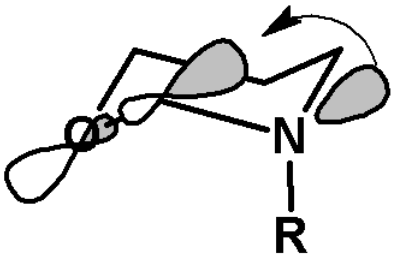

Source: The Author

4.3.2. Thermogravimetric Analysis (TGA)

In order to evaluate if the initial polymerization temperatures were too harsh to obtain the polybenzoxazines as intact as possible (without oxidation of alkyl chains), thermogravimetric analysis (TGA) of the saturated benzoxazines and cardanol were performed (Figure 24).

Figure 24 – TGA curves of saturated benzoxazines and cardanol: TGA (a) and DTGA (b)

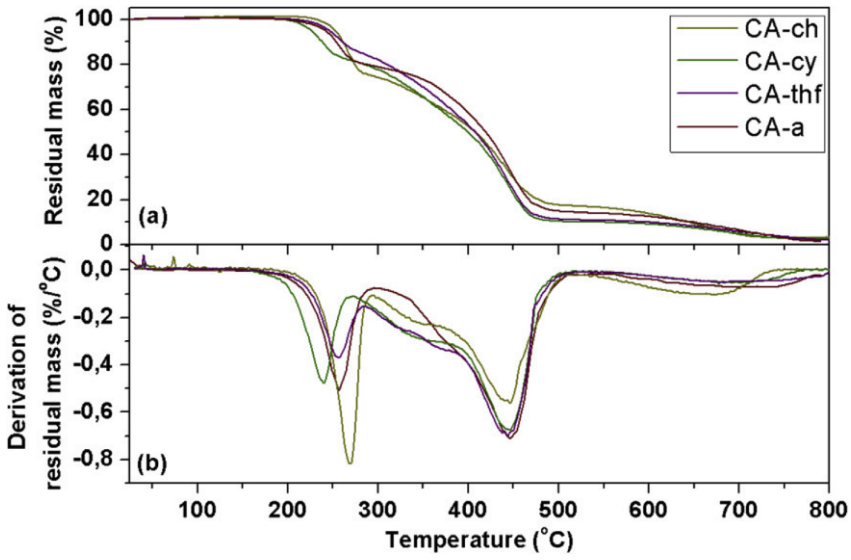

Source: The Author

In general, three defined events were observed in the thermograms of benzoxazines, being the first the most important.

In the temperature range of 120 to 320 °C, were observed mass losses about 23 to 30% of benzoxazines. These losses may indicate the degradation of the alkyl chains of the monomers, whereas in this same temperature range, cardanol (CA) is totally degraded (Figure 24). The reason why these first degradations of the benzoxazines occurs at higher temperatures than the saturated cardanol may be that, in these conditions, the monomers has already started the ring-opening polymerization to form a network, hindering further breakage of the long alkyl chains.

4.4. Polymerization of cardanol-based benzoxazines with catalysts

The use of catalyst for the polymerization of benzoxazines in lower temperatures has been studied. Caló and co-workers used phosphorus pentachloride (PCl_5) to polymerize at room temperature the first reported cardanol-based benzoxazine (CALÒ et al., 2007). Nevertheless, using PCl_5 as a catalyst is not easy to handle, as this compound is highly reactive with wet air and/or oxygen, making this catalyst not suitable for large-scale production. Other catalysts, like *p*-toluenesulfonates and lithium iodide, have been demonstrated to be very useful to polymerize benzoxazines at lower temperature without concerning about the use of inert atmosphere (LIU et al., 2011; WANG et al., 2013a).

As it was observed from TG analysis, the polymerization of cardanol-based benzoxazines needed to be conducted at lower temperature in order to obtain an intact cardanol moiety in the polymeric structure, in this sense, other catalysts were studied to increase the scope of choice. Using a concentration of 1% mol/mol of catalyst with the benzoxazine, DSC's were performed to understand the influences of the following polymerization promoters, which were: *p*-toluenesulfonic acid (*p*-TsOH), zinc chloride ($ZnCl_2$) and magnesium chloride ($MgCl_2$).

The DSC thermograms of the CA-a containing these catalysts (Figure 25) were summarized on Table 4. It was noticed that the use of catalyst provided a higher ΔH than CA-a itself. A possible explanation for this may be due the balance between the

heat absorption of the C-O bond and the heat release of the C-O cleavage. The catalyst could coordinate with oxygen atom, making the C-O bond more susceptible to be broken by a small amount of heat absorption. Combining the lower heat absorption with the same heat release explains the higher ΔH.

Figure 25 - DSC thermograms of CA-a without and with catalyst (1% mol/mol)

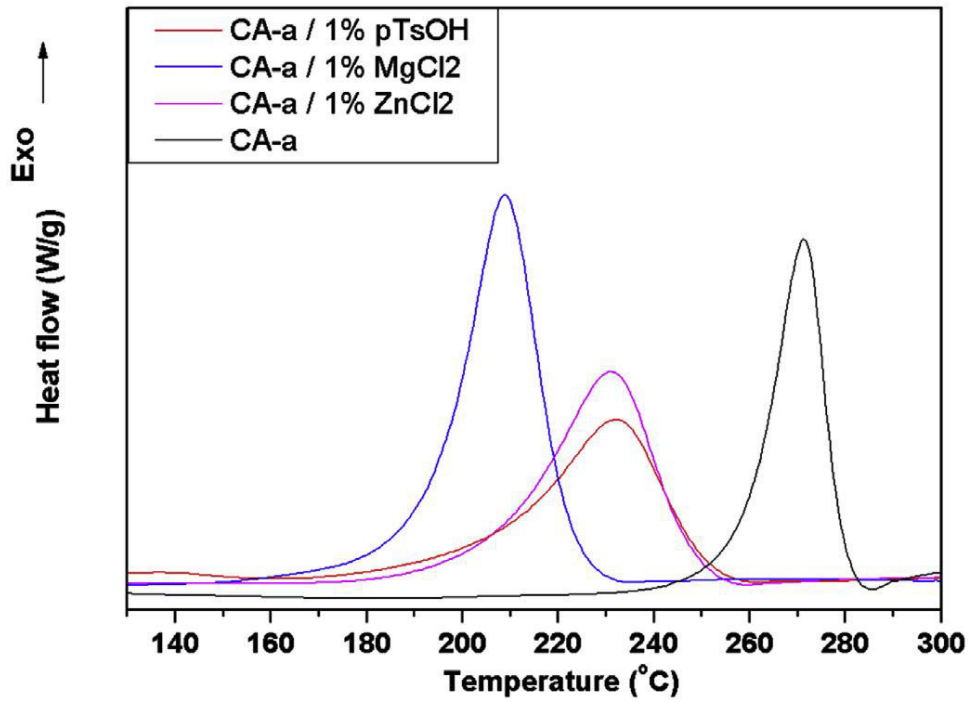

Source: The Author

Table 4 - Values obtained from the non-isothermal DSC thermograms of CA-a without and with catalyst (1% mol/mol)

Monomer	**T_e (°C)**	**T_p (°C)**	**ΔH (Jg^{-1})**
no catalyst	260.6	271.6	-90.9
$MgCl_2$	193.1	206.9	-146.1
$ZnCl_2$	207.1	228.7	-112.4
***p*-TsOH**	206.0	229.7	-100.0

Source: The Author

Among these catalysts, it was observed that the most suitable promoter is the cheap, abundant and innocuous $MgCl_2$, since this catalyst provided the highest ΔH with the lowest onset polymerization temperature. Higher concentrations of $MgCl_2$ were studied to analyse if the onset polymerization can be reduced even more. This was not the case as the DSC´s curves of the samples containing 3 and 5% of catalyst (Figure 26) showed that their initial polymerization temperatures and ΔH´s were almost the same as of the sample containing 1% of the catalyst.

Figure 26 - DSC thermograms of CA-a with $MgCl_2$

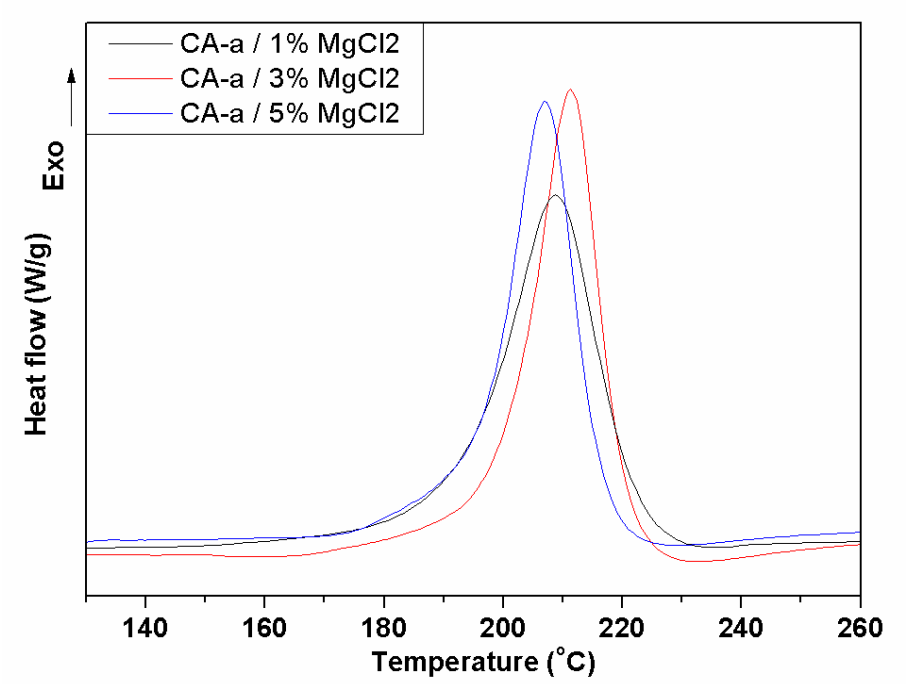

Source: The Author

Since the concentration increase of $MgCl_2$ didn´t reduced the onset polymerization temperature even more, and looking forward to use a minimum amount of the catalyst as possible, 1% of this promoter was chosen also to be employed for the polymerization of the other monomers. The DSC analyses of these benzoxazines with $MgCl_2$ were also performed (Figure 27) and the results are summarized on Table 5.

Figure 27 - DSC thermograms of cardanol-based benzoxazines with $MgCl_2$ (1% mol/mol)

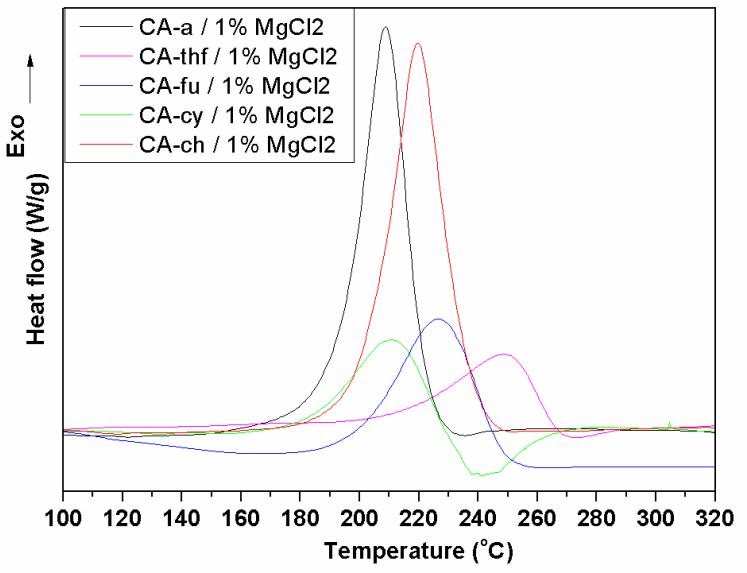

Source: The Author

Table 5 - Values obtained from the non-isothermal DSC thermograms of benzoxazines with MgCl2 (1% mol/mol)

Monomer	T_e (°C)	T_p (°C)	ΔH (Jg^{-1})
CA-a	192,8	207,1	-146,1
CA-ch	202,3	218,2	-163,9
CA-cy	185,6	207,3	-50,6
CA-fu	200,1	222,9	-80,2
CA-thf	217,1	246,3	-48,0

Source: The Author

It was noticed that the $MgCl_2$ reduced significantly the onset polymerization temperatures (T_e) of all benzoxazines (see Table 3 and 5). The T_e of CA-a and CA-ch were greatly reduced in about 67 °C. The initial polymerization temperatures of CA-cy, CA-fu and CA-thf were also reduced. The probable reason why the T_e of CA-thf was the less affected could be attributed to the basicity of the oxygen atom of the tetrahydrofuran ring that may also interact with $MgCl_2$, making the catalyst less

effective to interact with the oxygen atom of the oxazine ring. This could also explain why the T_e of CA-fu was lower than of CA-cy and higher than of CA-thf, since the lone electron pair of the oxygen of the furan group participates in the aromaticity, turning this oxygen less basic. It was also noticed a relaxation process in the range of 230 to 270 ^oC, right after the polymerization of CA-cy with $MgCl_2$.

The enthalpy of polymerization (ΔH) of these catalysed benzoxazines were overall higher than their blank ones. The ΔH of the aromatic benzoxazines, CA-a, CA-ch and CA-fu, increased by 55.2, 73.6 and 40.1 J/g, respectively. The aliphatic benzoxazines, CA-thf and CA-cy, showed a slightly increase, 9.1 and 4.4 J/g, respectively. This small reduction of the ΔH of CA-cy could be due the heat absorption of the relaxation process.

4.4.1. Isothermal polymerizations of cardanol-based benzoxazines by DSC

Since the onset polymerization temperatures are relatively close, isothermal polymerizations of these catalysed benzoxazines were performed at 150 ^oC, in order to analyse in details the polymerization behaviour of each monomer by DSC, FT-IR and GPC.

The DSC thermograms of the polymerization study of the cardanol-based benzoxazines are shown on Figure 28 to 32 and their data are summarized in Table 6.

Figure 28 - DSC thermograms of CA-a under different polymerization times

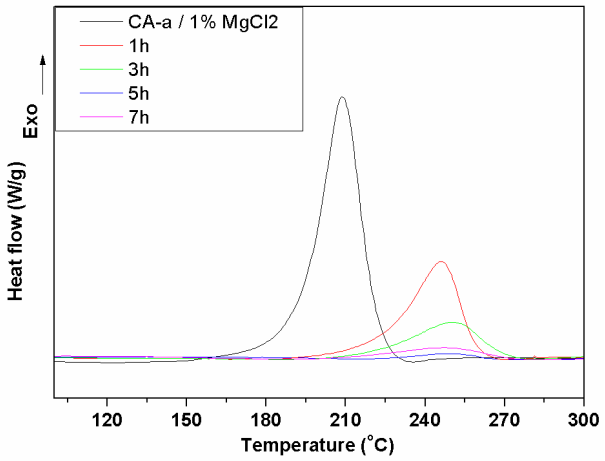

Source: The Author

Figure 29 - DSC thermograms of CA-ch under different polymerization times

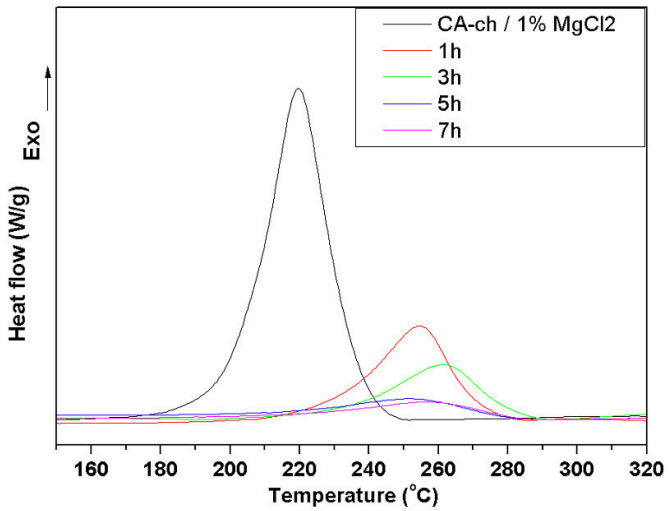

Source: The Author

Figure 30 - DSC thermograms of CA-cy under different polymerization times

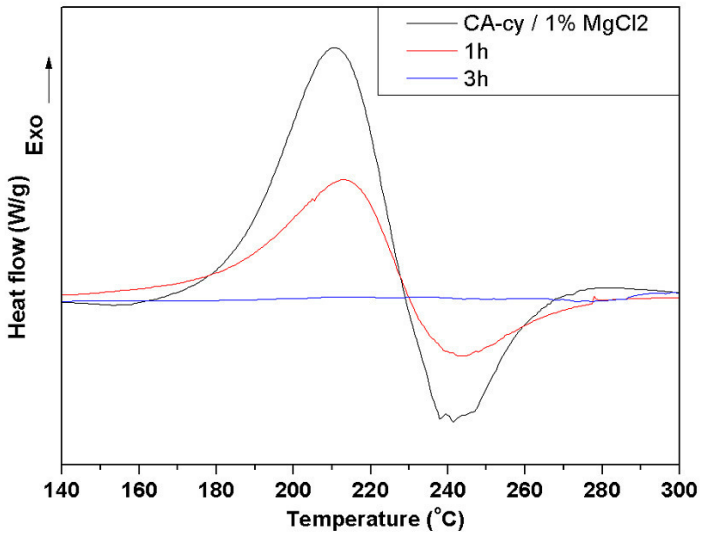

Source: The Author

Figure 31 - DSC thermograms of CA-fu under different polymerization times

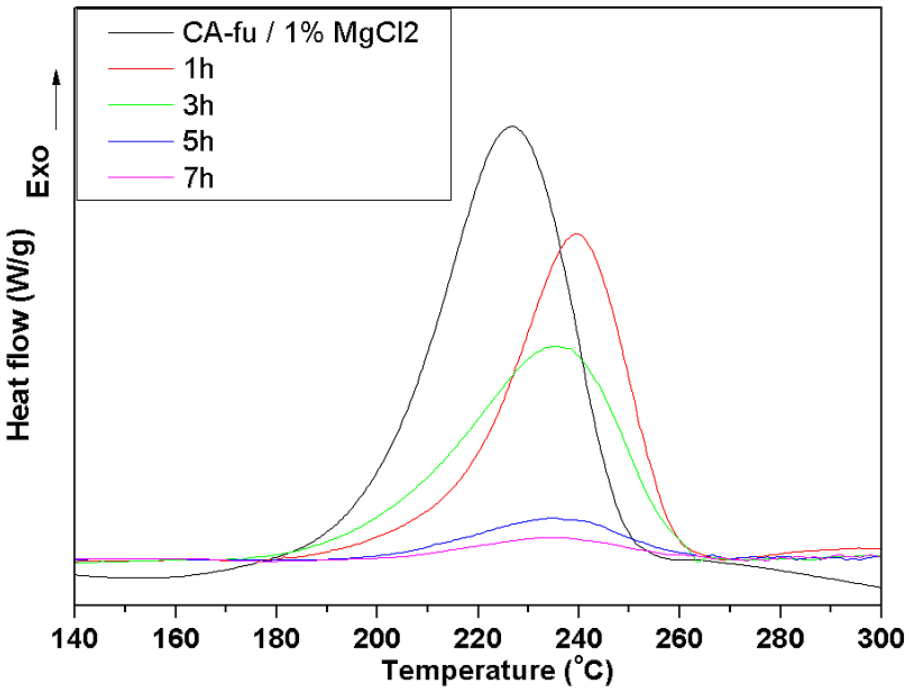

Source: The Author

Figure 32 - DSC thermograms of CA-thf under different polymerization times

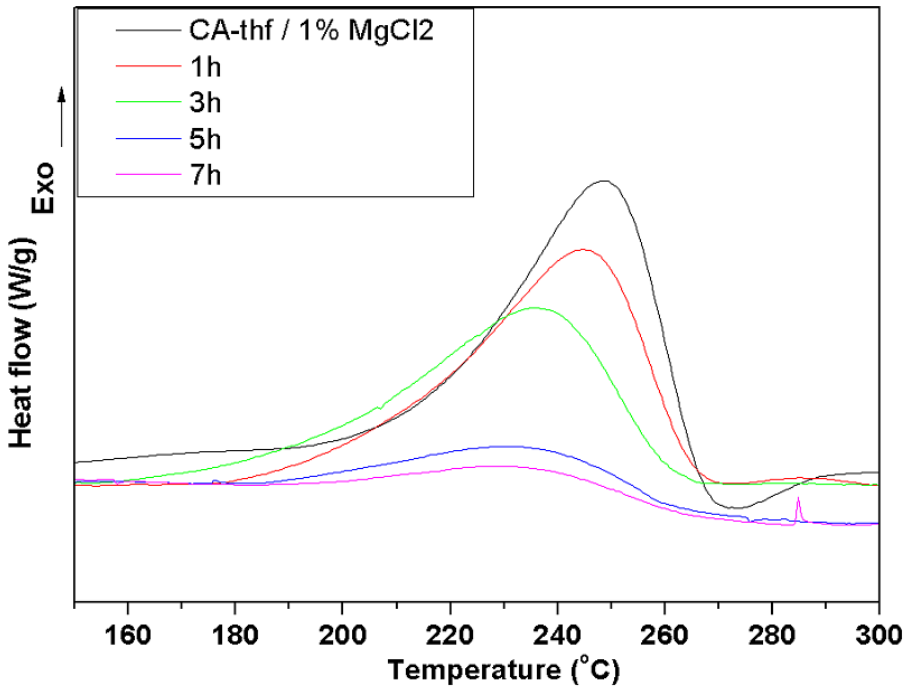

Source: The Author

Table 6 - Values obtained from isothermal DSC thermograms of benzoxazines with $MgCl_2$ (1% mol/mol) at 150 ºC

Benzoxazine	Monomer		1h		3h		5h		7h	
	T_e	ΔH	T_e	ΔH	T_e	ΔH	T_e	ΔH	T_e	ΔH
CA-a	193	-146	224	-75	224	-35	230	-5	220	-10
CA-ch	202	-164	230	-62	236	-36	229	-16	231	-13
CA-cy	186	-51	191	-25	---	---	---	---	---	---
CA-fu	200	-80	214	-60	200	-49	204	-10	204	-5
CA-thf	217	-48	207	-44	200	-36	203	-16	176	-8

Source: The Author

According to the DSC curves of CA-a, as the time increases during the isothermal polymerization of CA-a, it was observed that the T_e and the T_p also increased. The displacement of this exothermic event may be due the fact that the first formed oligomers have different heat capacity in relation to the monomers, and furthermore, with the increasing size of the oligomers, the interactions between oxazine units become more difficult, requiring much more energy to polymerize even further. As noted on the polymerization of CA-a, the DSC thermograms of CA-ch also showed the displacement of the exothermic event to higher temperatures. The DSC thermograms of CA-cy didn't show the displacement of the exothermic event, but demonstrated that at 3 hours the monomer was completely polymerized. The DSC thermograms of CA-fu showed a displacement of T_e to higher temperatures after 1 h of heating. But on the other hand, T_e of the 3h, 5h and 7h samples were reduced when compared with the 1h sample. This could mean that the first oligomers work as a thermal barrier for the other monomers, but from 3h and beyond the polymerization kinetic remained the same. The DSC thermograms of CA-thf, demonstrated that the exothermic event was generally maintained at the same temperature range as the time increased.

4.4.2. Isothermal polymerizations of cardanol-based benzoxazines by FT-IR

The polymerization of the cardanol-based benzoxazines was also studied by FT-IR spectroscopy, which showed to be an efficient tool to analyse the polymerization mechanism.

In the spectra of CA-a, the aniline derivative, (Figure 33), the absence of a broad band in the range of 3700 to 3100 cm^{-1}, as the polymerization time increases, indicated that the majority of the oligomers didn't possess a phenolic structure. The decrease of the band at 1228 cm^{-1} as the polymerization time increases indicated the partial cleavage of the C-O bond of the oxazine ring. The displacement of the band at 1499 cm^{-1} to 1488 cm^{-1} was also observed, indicating the transformation of the trisubstituted to the tetrasubstituted benzene ring as the polymerization time increased. It was also observed the disappearance of the band at 1576 cm^{-1} and the appearance of a signal at 1563 cm^{-1}, as the polymerization time increased. This displacement may be also related to the transformation of the trisubstituted to the tetrasubstituted ring.

Another interesting observation was the disappearance and the appearance of the bands at 1600 and 1590 cm^{-1}, respectively. According to the *Spectral Database for organic compounds SDBS* (NATIONAL INSTITUTE OF ADVANCED INDUSTRIAL SCIENCE AND TECHNOLOGY, 2015), most of the *ortho* alkyl-substituted aniline rings possess a C=C stretching band (e.g. *o*-ethylaniline, *N*-ethyl-*o*-toluidine and *N*,*N*-diethyl-*o*-toluidine) at around 1580 to 1590 cm^{-1}, while for the *para* alkyl substituted aniline rings (e.g. *p*-toluidine, *N*,*N*-diethyl-*p*-toluidine, *N*-ethyl-*p*-toluidine, and *N*,*N*-dimethyl-*p*-toluidine) it wasn´t found any band or sometimes it was found a very low intense band at this region. However, in the spectra of *o*-(phenyliminomethyl)phenol, a Schiff base analogue of CA-a, there is a very intense band at 1590 cm^{-1}. Thus, as it was mentioned before that the band at 1602 cm^{-1} indicated the C=C stretching of aniline groups among these benzoxazines, this displacement, from 1600 to 1590 cm^{-1}, could indicate an electrophilic substitution in *ortho* position of aniline ring. The selectivity for this position in an electrophilic substitution of aniline is also in line with Hehre and co-workers who demonstrated that, based on STO-3G calculations, the distribution of π-electrons of the orbitals at *ortho* position is higher than the distribution at *para* position (HEHRE; RADOM; POPLE, 1972). In any case, this same displacement can also be attributed to the conversion of CA-a into a Schiff base during the ring-opening polymerization (ROP) mechanism, reducing the C=C bond strength of the aniline group due the increase of its conjugation.

It was also observed the appearance of a band at 1658 cm^{-1} on the 1h sample and thereafter, which could indicate a C=O stretching of aryl carboxylic acid in *ortho* position of a *m*-cresol, e.g. 2-hydroxy-*p*-toluic acid (NATIONAL INSTITUTE OF

ADVANCED INDUSTRIAL SCIENCE AND TECHNOLOGY, 2015). Due to the intramolecular hydrogen bonding, bands of carbonyl groups in *ortho* position of phenols are of lower energy when compared in *para* position. This suggests that Ar-**CH_2**-N methylenes of some monomers may be susceptible to oxidation. The 3h sample showed also a band at 1671 cm^{-1}, which could be a characteristic of a C=O stretching of aryl aldehyde in *ortho* position of a phenol, e.g. salicylaldehyde (NATIONAL INSTITUTE OF ADVANCED INDUSTRIAL SCIENCE AND TECHNOLOGY, 2015). This explains why this band didn't remain at the 5h and 7h samples, indicating a possible conversion of an aryl aldehyde oxidating to an aryl carboxylic acid. The band at 1658 cm^{-1} was also observed by Yanfang and co-workers (LIU et al., 2013), but they related this band to the imine group of a Schiff base, which is, most likely, not the case, since no bands are observed in the range of 2700 to 1620 cm^{-1} on the spectra of *o*-(phenyliminomethyl)phenol and *o*-((p-chlorophenylimino)methyl)phenol (LIU et al., 2012, 2013).

Figure 33 - FT-IR spectra of CA-a with $MgCl_2$ (1% mol/mol) with different polymerization time at 150 ºC.

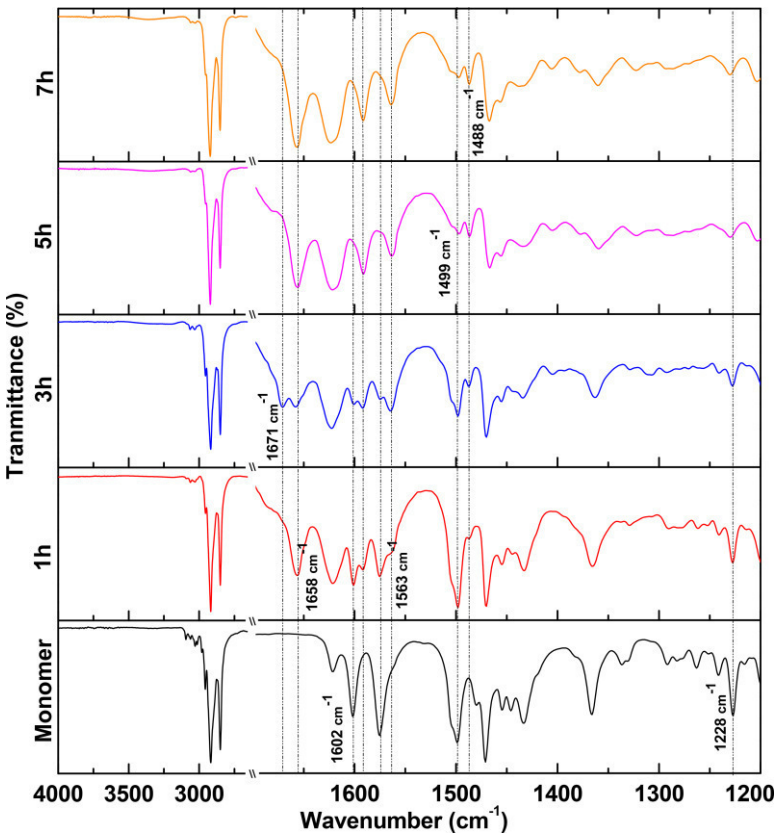

Source: The Author

As seen on the polymerization of CA-a, the FT-IR spectra of CA-ch (Figure 34) showed the progress of the polymerization by the cleavage of the oxazine ring observed at 1262 cm^{-1}, and the transformation of the trisubstituted to a tetrasubstituted benzene ring by bands at 1498 cm^{-1} and 1487 cm^{-1}, respectively. In addition, the C=C aniline-type band at 1597 cm^{-1} didn't suffer a displacement, but disappeared as the polymerization time increased. This could indicate that this aniline group didn't suffer an electrophilic substitution, which is understandable since the chlorine atom at *para* position deactivates the benzene ring. Another remark was the disappearance of the band at 1049 cm^{-1}, indicating that the C-Cl bond is being broken as the polymerization time increases. The sample of 5 hours of polymerization and thereafter didn´t show any presence of this bond. Here again, it was observed the oxidation of the Ar-**CH_2**-N methylenes by the appearance of bands at 1658 cm^{-1} and at 1671 cm^{-1}, in all the polymerized samples (1h-7h). As no bands are visualized at the hydroxyl region even after 7h, the polymer obtained should present a phenoxy structure.

Figure 34 - FT-IR spectra of CA-ch with $MgCl_2$ (1% mol/mol) with different polymerization time at 150 ºC.

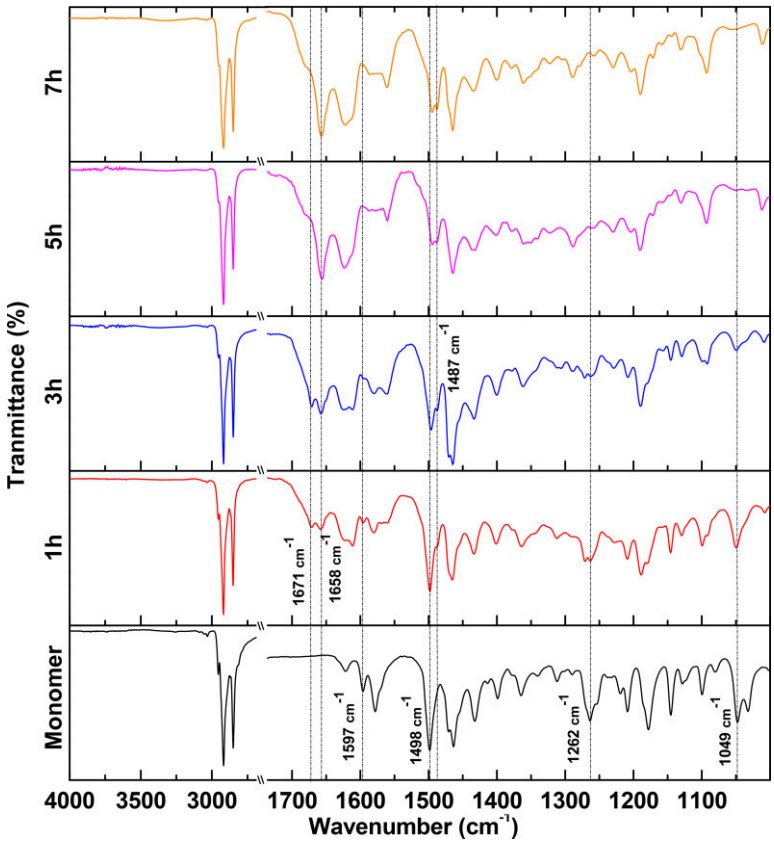

Source: The Author

The complete polymerization of CA-cy was also confirmed on the FT-IR spectra (Figure 35), showing that the sample of 3 hours of polymerization didn't had any presence of the C-O-C group at 1242 cm^{-1}, and the trisubstituted benzene ring at 1505 cm^{-1}. The disappearance of this band with the appearance of a "shoulder" was also shown on the spectra of the polymerization of benzoxazines containing aliphatic amines of Wang and co-workers, considering it as a tetrasubstituted benzene ring (WANG et al., 2014). It was also noticed that no bands were observed at around 1700 cm^{-1}, which would indicate any evidence of oxidation. This could mean that fast thermal polymerization can prevent oxidation on alkyl and Ar-**CH_2**-N methylene groups. The analysis of the 3h sample showed a broad band at around 3400 cm^{-1}, indicating that, in this case, the phenolic structure of the polymer is formed preferentially.

Figure 35 - FT-IR spectra of CA-cy with $MgCl_2$ (1% mol/mol) with different polymerization time at 150 ºC

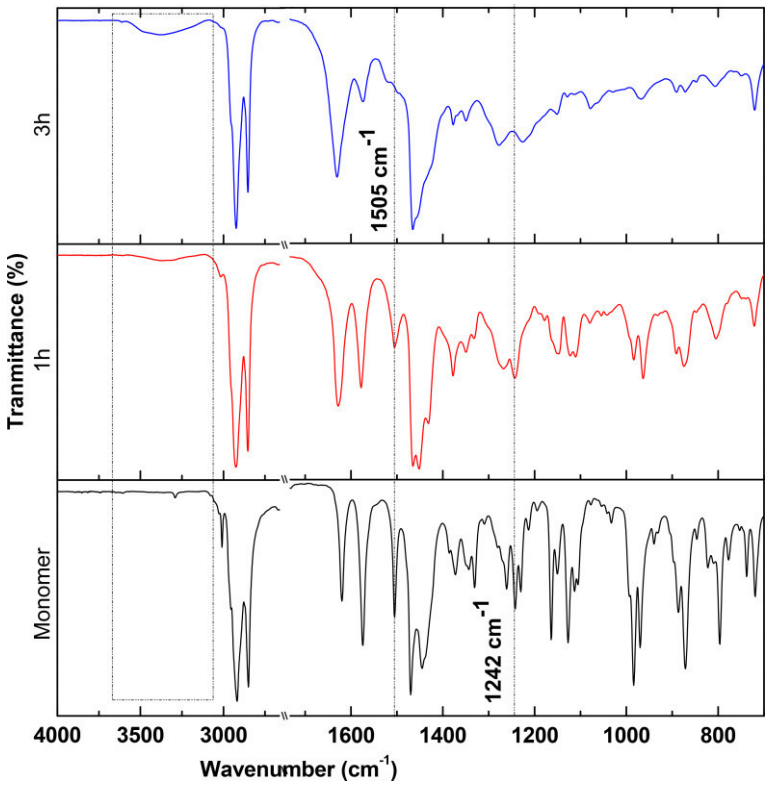

Source: The Author

Even though the DSC confirms that only a little quantity of the CA-fu monomers remained in the 7 h sample, it was observed on the FT-IR spectra (Figure 36), that as the polymerization time increases, the decreasing of the C-O-C group by the band at 1247 cm^{-1} wasn't so easy to track. This band is near another one at 1242 cm^{-1}, which remained intact until the 7 h sample, and which could represent the C-O-C group of the furan ring. Unlike the previous benzoxazines containing aromatic amines, the band regarding the trisubstituted benzene ring didn't disappear. The band at 1506 cm^{-1} is maintained throughout the polymerization time, which can be assumed that the electrophilic substitution occurred directly on the furan ring instead of the phenolic ring. Since the furfuryl group possesses different conformers, the furan is favoured to suffer electrophilic substitution than the cardanol's phenolic ring, which is less reactive due the steric hindrance by the long alkyl side-chain. Due the small intensity of the hydroxyl region and the integrity of the tri-substituted band, the polymer can also possess phenoxy structure. The oxidation of the Ar-**CH_2**-N methylenes was also observed from the 1h to the 7h samples by the appearance of a new band at 1658 cm^{-1}.

Figure 36 - FT-IR spectra of CA-fu with $MgCl_2$ (1% mol/mol) with different polymerization time at 150 ºC.

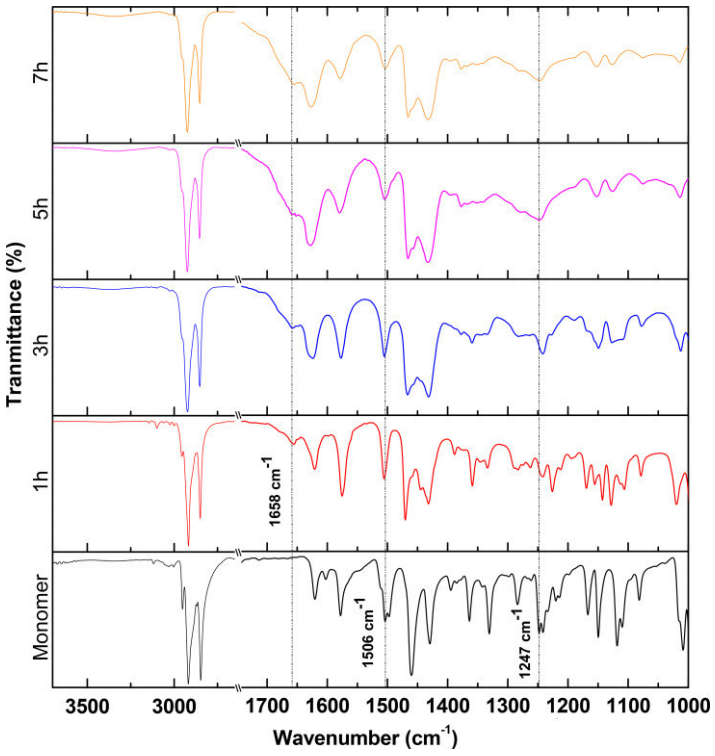

Source: The Author

In the FT-IR spectra of CA-thf (Figure 37), the decrease of the band at 1245 cm^{-1} indicated the opening the oxazine ring. The decrease of the band at 1507 cm^{-1} was observed as the polymerization time increased, meaning that the monomers (trisubstituted benzene rings) are being consumed during this process. The band at 1063 cm^{-1}, which refers to the C-O-C asymmetric stretching of the tetrahydrofuran group, remained during the whole polymerization. A broad band region at around 1700 to 1650 cm^{-1} indicated different kinds of oxidation reactions occurring during the polymerization of the benzoxazine. Even though that the five benzoxazines were polymerized simultaneously at the same temperature, it was clear that the temperature employed was too harsh to polymerize the monomer. As the onset polymerization temperature of this monomer with catalyst was the highest, the polymerization occurred slower, making this polymer more exposed to oxidation.

Figure 37 - FT-IR spectra of CA-thf with MgCl2 (1% mol/mol) with different polymerization time at 150 ºC.

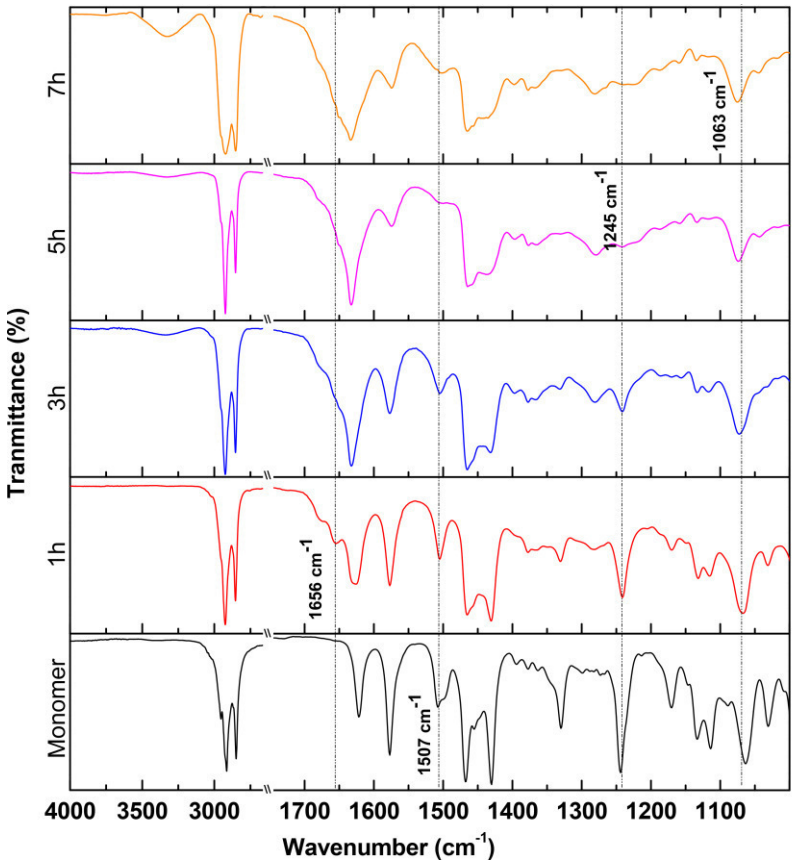

Source: The Author

4.4.3. Isothermal polymerizations of cardanol-based benzoxazines by GPC

Since one of the objectives of this work was to evaluate the profile of thermoplastic cardanol-based polybenzoxazines, a gel permeation chromatography analysis was fundamental to know the distribution size/weight of the oligomers obtained.

The molecular weight distributions of the latest polymerized benzoxazines (3 h for CA-cy and 7 h for the rest) were obtained using GPC analysis and their data were summarized on Table 7.

Table 7 - Summary of the values of the GPC analysis of the latest polymerized benzoxazines.

Polymer	***Polym. Time (h)***	$\bar{M}_n$ ***(g/mol)***	$\bar{M}_w$ ***(g/mol)***	***PDI*** $(\bar{M}_w/\bar{M}_n)$	x_n	x_w
Poly(CA-a)	**1**	1093	1692	1.5	2.6	4.0
	3	968	1331	1.4	2.3	3.2
	5	1341	4588	3.4	3.2	10.9
	7	1404	4041	2.9	3.3	9.6
Poly(CA-ch)	**1**	985	1352	1.4	2.2	3.0
	3	994	1438	1.4	2.2	3.2
	5	1498	4508	3.0	3.3	9.9
	7	1447	4125	2.9	3.2	9.1
Poly(CA-cy)	**1**	1260	2053	1.6	2.9	4.8
	3	2313	20302	8.8	5.4	47.5
Poly(CA-fu)	**1**	1059	1511	1.4	2.5	3.6
	3	1378	2619	1.9	3.2	6.2
	5	2833	11687	4.1	6.7	27.5
	7	1770	8185	4.6	4.2	19.2
Poly(CA-thf)	**1**	811	906	1.1	1.9	2.1
	3	1199	2176	1.8	2.8	5.1
	5	1468	3163	2.2	3.4	7.4
	7	1183	3782	3.2	2.8	8.8

Source: The Author

According to the polydispersity indices (PDI), these polymers showed to be very polydispersed. Poly(CA-a), Poly(CA-ch) and Poly(CA-thf) demonstrated to possess similar chain lengths, in which the number-average degree of polymerization (x_n) suggest the formation of trimeric structures, while weight-average (M_w) and degree of polymerization (x_w) indicate the formation of nonomers. But in these parameters, the influence of high molar mass molecules is higher and the x_w values can be overestimated. To the calculation of $\overline{M}_n$, the influence of each molecule is the same, independent on it dimension, and the x_n is a more representative value. The number-average molar mass of poly(CA-thf) is slightly lower than $\overline{M}_n$ values for poly(CA-a) and poly(CA-ch). Those three oligomers showed similar polydispersity index. For Poly(CA-fu), the average oligomer molecule is constituted of about four units. Poly(CA-cy) demonstrated a very high PDI with a chain length composed by approximately five monomers. The PDI value of CA-cy is the highest among the benzoxazines, indicating that this polymer is more heterogeneous than the others.

These discrepant molecular weight values of Poly(CA-cy), could be related to the fast polymerization of the monomer (3h), as seen on the DSC thermograms (Figure 13), and also to the absence of oxidative processes, as seen on the FT-IR spectra (Figure 16), making it clear that the low T_e under catalysed conditions enabled an effective and mild polymerization of the monomer.

4.4.4. Proposed oligomeric structures

In this section will be proposed the structures of each polybenzoxazine, by taking into account the data obtained by DSC, FT-IR and the number average molar weight ($\overline{M}_n$) of the GPC of the latest polymerized samples.

Figure 38 - Proposed structure of Poly(CA-a)

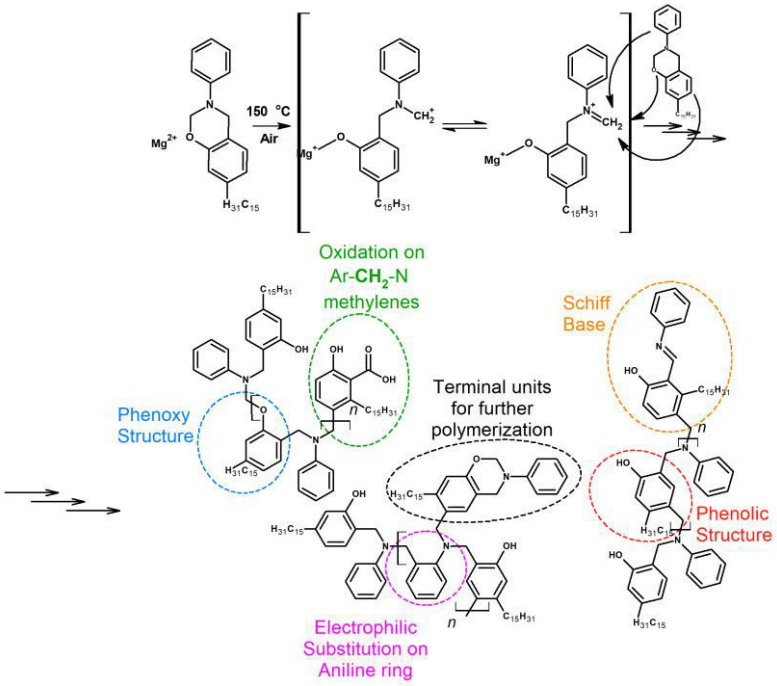

Source: The Author

Figure 39 - Proposed structure of Poly(CA-ch)

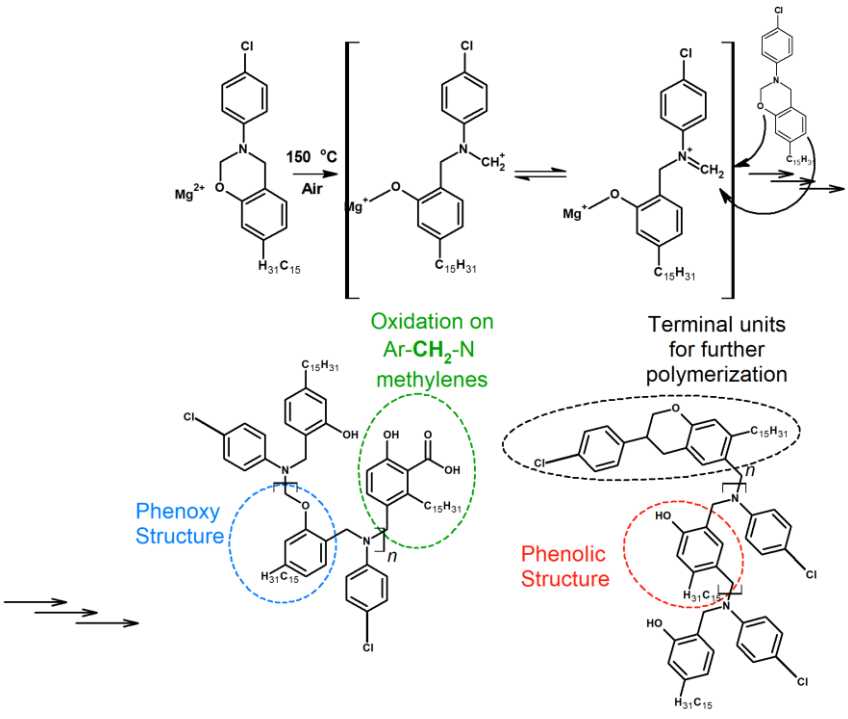

Source: The Author

Figure 40 - Proposed structure of Poly(CA-cy)

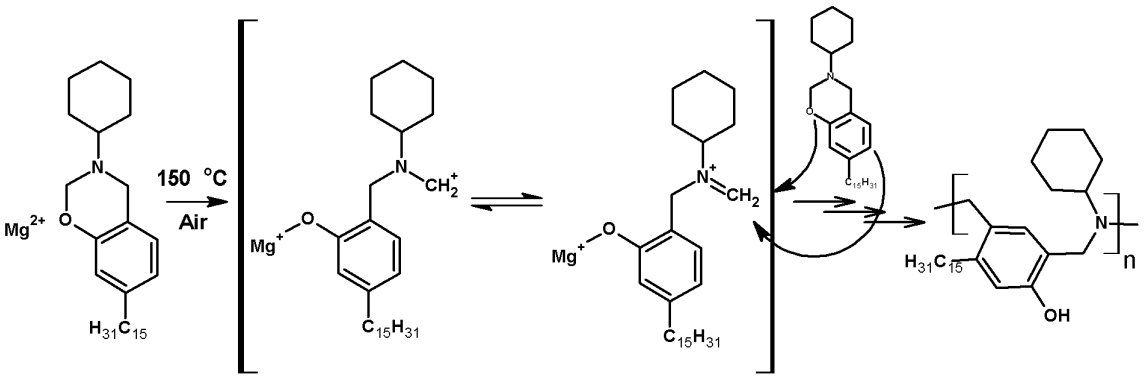

Source: The Author

Figure 41 - Proposed structure of Poly(CA-fu)

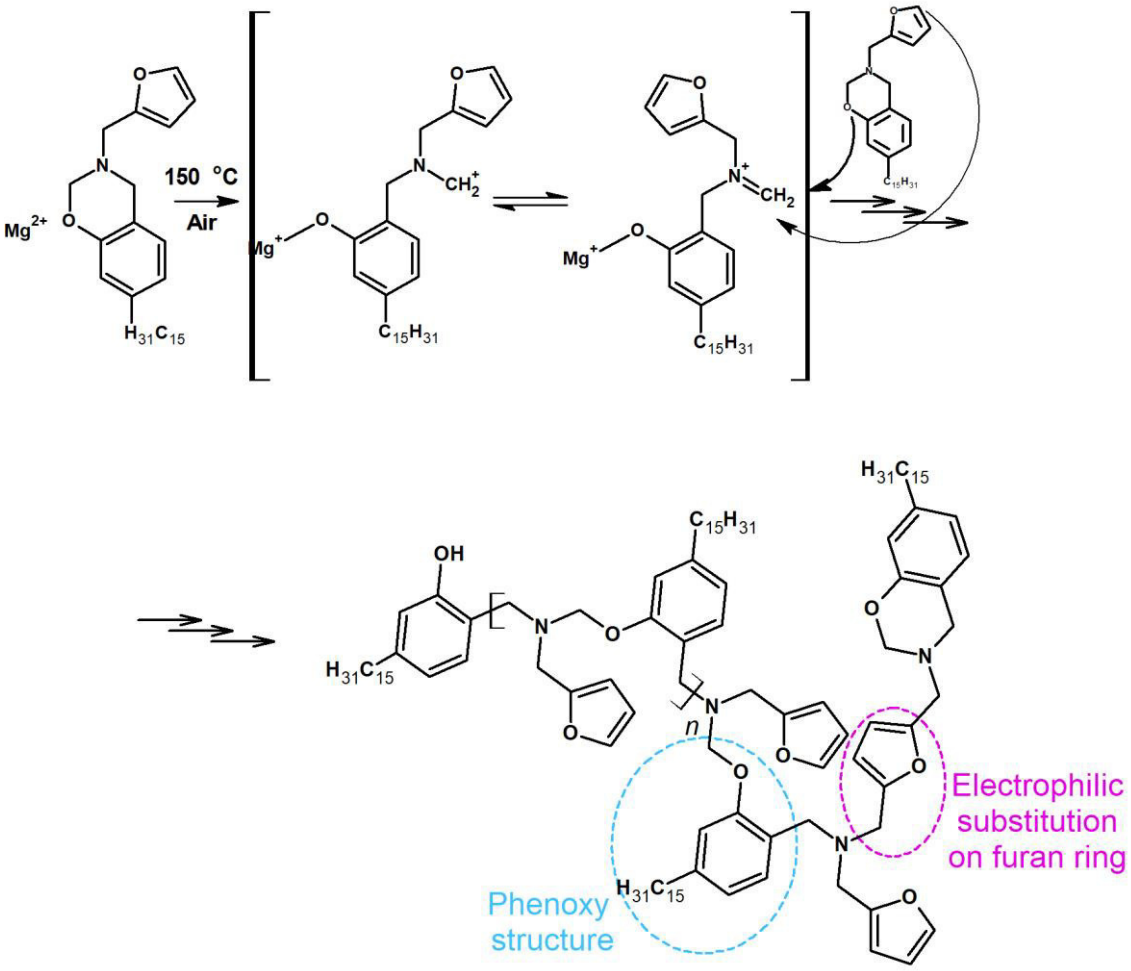

Source: The Author

Figure 42 - Proposed structure of Poly(CA-thf)

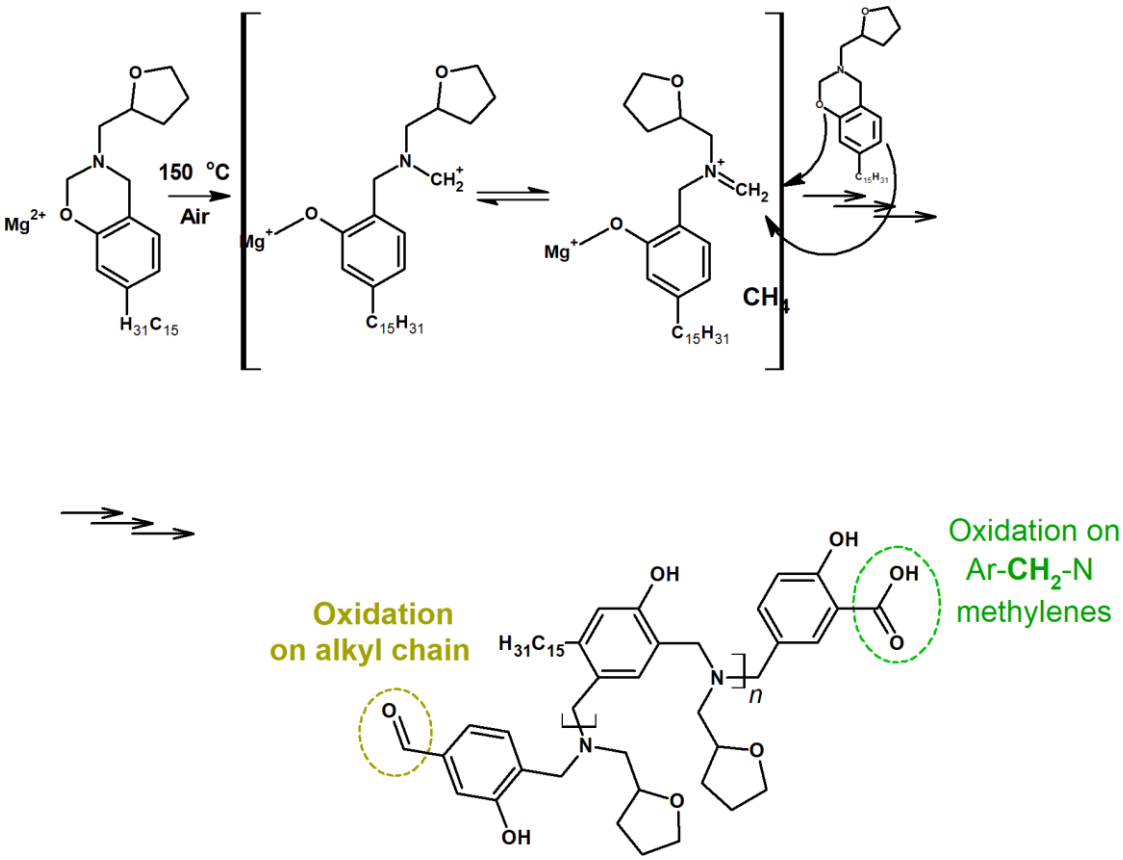

Source: The Author

5. CONCLUSION

This study gives a better understanding how primary amines act upon the properties of cardanol-based benzoxazines. It was observed on the ^{1}H and the ^{13}C NMR spectra how the oxazinic atoms present different chemical shifts depending on the type of primary amine used. On the FT-IR spectra was observed at which wavenumber it was possible to find the two most observed bands regarding the C-O-C group of the oxazinic ring and the C=C stretching of a trisubstituted benzene ring, depending on the primary amine used. Through DSC analyses, it was demonstrated how different primary amines influence the stability of the oxazine ring. After the cleavage of the oxazine ring, the more the formed carbocation is stabilized by the amine lone pair, the lower the onset polymerization temperature.

In order to polymerize the benzoxazines at low temperatures (below 200 ºC), magnesium chloride demonstrated to be a very good catalyst for the polymerization of cardanol-based benzoxazines. It was clear that the basicity of the substituent of the amine group influences on the effectiveness of the catalyst. Following the polymerization of the cardanol-based benzoxazines by FT-IR, it was also observed that the Ar-CH_2-N methylenes might be susceptible to suffer oxidation during the polymerization, except of CA-cy.

There is no doubt that with a better comprehension of the oligomerization characteristics and the influence of primary amines in the preparation of thermoplastic cardanol-derived polybenzoxazine, it will be much easier not only to synthesize a specific monomer based on its application, but it will also expand the utilization of this class of polymer, which is basically known for its use as thermoset material. In any case, further studies are required to understand better the relationships between: the onset polymerization temperature and the molecular weights of the polymer; the influence of the catalyst on the polymer structures; and, the oxidation processes that might occur during the polymerization.

REFERENCES

AKHTER, M. et al. Synthesis of some new 3,4-dihydro-2H-1,3-benzoxazines under microwave irradiation in solvent-free conditions and their biological activity. **Medicinal Chemistry Research**, v. 20, n. 8, p. 1147–1153, 2011.

ANASTAS, P. T.; WARNER, J. C. **Green Chemistry: Theory and Practice**. New York: Oxford University Press, 1998.

ATTANASI, O. A. et al. Solvent Free Synthesis of Novel Mono- and Bis-Benzoxazines from Cashew Nut Shell Liquid Components. **Current Organic Chemistry**, v. 16, n. 21, p. 2613–2621, 2012.

BARANEK, A. D. et al. Flexible aliphatic-bridged bisphenol-based polybenzoxazines. **Polymer Chemistry**, v. 3, n. 10, p. 2892–2900, 2012.

BARROSO, S. et al. Three-Component Mannich Couplings En Route to Substituted Aminophenol and Benzoxazine Derivatives. **Synlett**, v. 2010, n. 16, p. 2425–2428, 2010.

CALÒ, E. et al. Synthesis of a novel cardanol-based benzoxazine monomer and environmentally sustainable production of polymers and bio-composites. **Green Chemistry**, v. 9, n. 7, p. 754–759, 2007.

CHIOU, K.; ISHIDA, H. Incorporation of Natural Renewable Components and Waste Byproducts to Benzoxazine Based High Performance Materials. **Current Organic Chemistry**, n. 17, p. 913–925, 2013.

DENG, Y. et al. Influence of substituent on equilibrium of benzoxazine synthesis from Mannich base and formaldehyde. **Physical Chemistry Chemical Physics**, v. 16, n. 34, p. 18341, 2014a.

DENG, Y. et al. Kinetics of 3,4-Dihydro-2H-3-phenyl-1,3-benzoxazine Synthesis from Mannich Base and Formaldehyde. **Industrial & Engineering Chemistry Research**, v. 53, n. 5, p. 1933–1939, 2014b.

DUMAS, L. et al. Facile preparation of a novel high performance benzoxazine–CNT based nano-hybrid network exhibiting outstanding thermo-mechanical properties. **Chemical Communications**, v. 49, n. 83, p. 9543–9545, 2013.

DUNKERS, J.; ISHIDA, H. Vibrational assignments of N,N-bis(3,5-dimethyl-2-hydroxybenzyl)methylamine in the fingerprint region. **Spectrochimica Acta Part A: Molecular and Biomolecular Spectroscopy**, v. 51, n. 5, p. 855–867, 1995.

FAO. Disponível em: <http://faostat3.fao.org/faostat-gateway/go/to/browse/Q/QC/E>. Acesso em: 30 ago. 2015.

GARG, V. et al. Synthesis, biological evaluation and molecular docking studies of 1,3-benzoxazine derivatives as potential anticancer agents. **Medicinal Chemistry Research**, v. 22, n. 11, p. 5256–5266, 2013.

HEHRE, W. J.; RADOM, L.; POPLE, J. A. Molecular orbital theory of the electronic structure of organic compounds. XII. Conformations, stabilities, and charge distributions in monosubstituted benzenes. **Journal of the American Chemical Society**, v. 94, n. 3, p. 1496–1504, 1972.

HOLLY, F. W.; COPE, A. C. Condensation Products of Aldehydes and Ketones with o-Aminobenzyl Alcohol and o-Hydroxybenzylamine. **Journal of the American Chemical Society**, v. 66, n. 11, p. 1875–1879, 1944.

HUNTSMAN. **Benzoxazines**. Disponível em: <http://www.huntsman.com/advanced_materials/a/Our Technologies/High Performance Components/Imides and Benzoxazines/Benzoxazines>. Acesso em: 24 jan. 2016.

ISHIDA, H.; AGAG, T. Handbook of Benzoxazine Resins. In: ISHIDA, H.; AGAG, T. (Eds.). . **Handbook of Benzoxazine Resins**. Oxford: Elsevier, 2011. Chapter 1

ISHIDA, H.; RODRIGUEZ, Y. Curing kinetics of a new benzoxazine-based phenolic resin by differential scanning calorimetry. **Polymer**, v. 36, n. 16, p. 3151–3158, 1995.

KATHALEWAR, M.; SABNIS, A.; D'MELO, D. Polyurethane coatings prepared from CNSL based polyols: Synthesis, characterization and properties. **Progress in Organic Coatings**, v. 77, n. 3, p. 616–626, 2014.

LI, S. et al. Synthesis, characterization, and polymerization of brominated benzoxazine monomers and thermal stability/flame retardance of the polymers generated. **Polymers for Advanced Technologies**, v. 21, n. 4, p. 229–234, 2010.

LI, W. et al. Preparation of novel benzoxazine monomers containing ferrocene moiety and properties of polybenzoxazines. **Polymer**, v. 53, n. 6, p. 1236–1244, 2012.

LI, X.; LUO, X.; GU, Y. A novel benzoxazine/cyanate ester blend with sea-island phase structures. **Physical Chemistry Chemical Physics**, v. 17, n. 29, p. 19255–19260, 2015.

LIU, C. et al. Mechanistic studies on ring-opening polymerization of benzoxazines: A mechanistically based catalyst design. **Macromolecules**, v. 44, n. 12, p. 4616–4622, 2011.

LIU, J.; ISHIDA, H. Anomalous Isomeric Effect on the Properties of Bisphenol F-based Benzoxazines: Toward the Molecular Design for Higher Performance. **Macromolecules**, v. 47, n. 16, p. 5682–5690, 2014.

LIU, Y. et al. Thermally activated polymerization behavior of bisphenol-S/methylamine-based benzoxazine. **Journal of Applied Polymer Science**, v. 124, n. 1, p. 813–822, 2012.

LIU, Y. et al. Thermal degradation behavior and mechanism of polybenzoxazine based on bisphenol-S and methylamine. **Journal of Thermal Analysis and Calorimetry**, v. 112, n. 3, p. 1213–1219, 2013.

LIU, Y. et al. Structural effects of diamines on synthesis, polymerization, and properties of benzoxazines based on o-allylphenol. **Polymer**, v. 57, p. 29–38, 2015.

LOCHAB, B.; VARMA, I. K.; BIJWE, J. Cardanol-based bisbenzoxazines. **Journal of Thermal Analysis and Calorimetry**, v. 107, n. 2, p. 661–668, 26 ago. 2011.

LOMONACO, D. et al. Study of technical CNSL and its main components as new green larvicides. **Green Chemistry**, v. 11, n. 1, p. 31–33, 2009.

LOMONACO, D. et al. Thermal studies of new biodiesel antioxidants synthesized from a natural occurring phenolic lipid. **Fuel**, v. 97, p. 552–559, 2012.

MARTINEZ, C. R.; IVERSON, B. L. Rethinking the term “pi-stacking”. **Chemical Science**, v. 3, n. 7, p. 2191–2201, 2012.

MOHAPATRA, S.; NANDO, G. B. Cardanol: a green substitute for aromatic oil as a plasticizer in natural rubber. **RSC Adv.**, v. 4, n. 30, p. 15406–15418, 2014.

NATIONAL INSTITUTE OF ADVANCED INDUSTRIAL SCIENCE AND TECHNOLOGY. **SDBSWeb**. Disponível em: <http://sdbs.db.aist.go.jp>. Acesso em: 12 nov. 2015.

RAO, B. S.; PATHAK, S. K. Thermal and viscoelastic properties of sequentially

polymerized networks composed of benzoxazine, epoxy, and phenalkamine curing agents. **Journal of Applied Polymer Science**, v. 100, n. 5, p. 3956–3965, 2006.

RUSSELL, V. M. et al. Study of the characterization and curing of a phenyl benzoxazine using15N solid-state nuclear magnetic resonance spectroscopy. **Journal of Applied Polymer Science**, v. 70, n. 7, p. 1401–1411, 1998.

SETHURAMAN, K.; ALAGAR, M. Thermo-mechanical and dielectric properties of graphene reinforced caprolactam cardanol based benzoxazine–epoxy nanocomposites. **RSC Advances**, v. 5, n. 13, p. 9607–9617, 2015.

SHARMA, P. et al. Microencapsulated cardanol derived benzoxazines for self-healing applications. **Materials Letters**, v. 133, p. 266–268, 2014.

SINI, N. K.; BIJWE, J.; VARMA, I. K. Renewable benzoxazine monomer from Vanillin: Synthesis, characterization, and studies on curing behavior. **Journal of Polymer Science, Part A: Polymer Chemistry**, v. 52, n. 1, p. 7–11, 2014.

TAWADE, B. V. et al. Processable aromatic polyesters based on bisphenol derived from cashew nut shell liquid: synthesis and characterization. **Journal of Polymer Research**, v. 21, n. 12, p. 617 (5-10), 2014.

THE WORLD BANK. **The World Bank**. Disponível em: <http://data.worldbank.org/?display=default>. Acesso em: 20 mar. 2016.

THIRUKUMARAN, P.; SHAKILA, A.; MUTHUSAMY, S. Synthesis and characterization of novel bio-based benzoxazines from eugenol. **RSC Advances**, v. 4, n. 16, p. 7959–7966, 2014.

VOIRIN, C. et al. Functionalization of cardanol: towards biobased polymers and additives. **Polymer Chemistry**, v. 5, p. 3142–3162, 2014.

WANG, C. et al. Synthesis and copolymerization of fully bio-based benzoxazines from guaiacol, furfurylamine and stearylamine. **Green Chemistry**, v. 14, n. 10, p. 2799–2806, 2012.

WANG, C. et al. Synthesis and thermal properties of a bio-based polybenzoxazine with curing promoter. **Journal of Polymer Science Part A: Polymer Chemistry**, v. 51, n. 9, p. 2016–2023, 2013a.

WANG, D. et al. Triazine-containing benzoxazine and its high-performance polymer.

Journal of Applied Polymer Science, v. 127, n. 1, p. 516–522, 2013b.

WANG, J. et al. Synthesis, curing behavior and thermal properties of fluorene-containing benzoxazines based on linear and branched butylamines. **Reactive and Functional Polymers**, v. 74, p. 22–30, 2014.

WANG, M.-Z. et al. Synthesis and Fungicidal Activity of Novel Aminophenazine-1-carboxylate Derivatives. **Journal of Agricultural and Food Chemistry**, v. 58, n. 6, p. 3651–3660, 2010.

ZHANG, C. et al. Thermal and dielectric properties of epoxy/DDS/CTBN adhesive modified by cardanol-based benzoxazine. **Journal of Adhesion Science and Technology**, v. 29, n. 8, p. 767–777, 2015.

ZHANG, H. et al. A novel polybenzoxazine containing styrylpyridine structure via the Knoevenagel reaction. **Journal of Applied Polymer Science**, v. 131, n. 19, p. 40823 (1-7), 2014.